University of Stavanger

FACULTY OF SCIENCE AND TECHNOLOGY

MASTER'S THESIS

Study program/specialization: MSc Biological Chemistry	Spring/Autumn semester, 2019
Author: Shanawar Ali Khan	Shanawar Ali Khan (Signature of author)
Program coordinator: Supervisor(s): Prof. Peter Ruoff	
Title of Master thesis: Computational evaluation of different arrangements for the circadian clock in *Arabidopsis thaliana*.	
Credits (ECTS): 60	
Keywords: Arabidopsis thaliana, Circadian Clock, Homeostasis, Computational model	Number of pages: 79 Supplemental material/other: Stavanger, Date/year: 15/06/2019

Acknowledgement

I would like to thank Prof. Peter Ruoff for his continuous assistance and encouragement throughout this thesis. His notable and gracious benefits were of numerous values through word and perception. I express my appreciation for his gentle assistance and support during many challenging periods in study

Secondly, I am grateful to our Co-Supervisor Behzad Heidari for his guidance in the discussions and searching for the literature to carry out research leading to completion of this thesis.

I offer my regards to my parents for their deep affection and motivational support in all the challenges that I have been through in my life.

Lastly, I am also thankful to my fellow master student Muhammad Harris, for practical help during writing of thesis.

Abstract

The circadian clock is an endogenous timekeeper that enables individuals to predict and adjust to their environment's regular differences between light and dark and high and low temperatures. This biological timing mechanism enables the organism coordinate evolutionary and metabolic occurrences to the best time of the day. Such a system is of significant value to plants as they cannot alter their place when the climate becomes detrimental as opposed to animals. The plant clock is a sophisticated system of interwoven feedback loops. Mathematical modeling methods have been used over the past few decades to comprehend the clock's internal functioning in the Arabidopsis thaliana model plant. These attempts have generated a range of increasingly complex designs. Here, a review of the research is presented which is done in order to find out the molecular machinery responsible for circadian rhythms. Along with this, a simple model and alterations in this model are conducted to check out the impact of such changes on phases as well as period of rhythms. An effort is also done to show comparison of model in relation to the findings presented in previous research. We are proposing an applicant model centered on LSODE optimization sub-routine calculation.

Table of Contents

Abbreviations

PRC	Phase response curve
WC	White collar gene
FRQ	Frequency gene
FRH	FRQ-interacting RNA helicase
TOC1	Timing of CAB expression 1
CCA1	Circadian clock associated 1
LHY	Late elongated hypocotyl
LUC	Luciferase
CAB2	Chlorophyll A/B binding protein
ZTL	Zeitlupe
GI	Gigantea
CDF	Cyclic dof factor 1
FKF1	

List of Figures

Aim of Thesis

As a result of the earth's rotation, rhythmic oscillations in ambient conditions have a substantial impact on the metabolism, physiology and conduct of most organisms. Circadian clocks have developed as molecular timekeeping systems that allow organisms to anticipate and predict these periodic changes in their surroundings such as light-dark cycles and temperature perturbations. Circadian rhythms make this possible that the allocation of resources and fitness enhancement to be effectively achieved — found that despite their independent evolutionary origins, eukaryotic clocks depend on transcription and translation - based feedback loops. In this study, we discuss current knowledge about how the external environment sets the clock pace and incorporate recent advances in understanding the molecular mechanisms that form the oscillator in the *Arabidopsis thaliana* model plant. The thesis is focused on the investigation of the organization of the plant circadian clock considering previously done studies. Development of model and testing the outcomes with relevance to the research done is also conducted. Certain changes made in subsequent models to check influence of different components and their pairing with one another. As the modifications are made based on the previous research, so it was considered justified writing a review of model development for *Arabidopsis thaliana*. The model developed especially in about the last two decades are also made part of this thesis in order to present a brief insight into the progress of research conducted by other scientific groups.

1 Introduction

1.1 Research for Circadian Rhythms

Organisms through evolutionary processes have developed mechanisms to determine time perception. This recognition of time exists for time changes during a day as well as during the whole year. The activities generally repeated during time duration of about 24 hours are termed circadian rhythms, and hence this short-term timing clock is termed circadian clock. The word "circadian" was coined by Franz Halberg in the 1950s, from the Latin words "circa" (about) and "dies" (day). Several biological processes are rhythmic during a period of a day, a month or even a complete year such as hormone synthesis, leaf movement, flowering, metabolic pathways and gene synthesis.

Circadian rhythms persist whether the organism is transferred into continuous light or darkness. Synchronization or entrainment to the day-night cycle by environmental cues and temperature compensation to a wide range of fluctuations are among the characteristics of circadian rhythms. The phenomenon that rhythms are intertwined and continue to operate even in the absence of any environmental stimuli first came under the observation. Leaf movement was the first observed clock phenotype, as noted by the French astronomer Jean Jacques d'Ortous de Marian, who observed the continuous movement of leaves on Mimosa placed in constant darkness in 1729 (1). This phenomenon, however, was not supposed to be associated with natural rhythms (1). During the day and night, Mimosa was known to open and close her leaves. For days, de Mairan put the plant in total darkness and observed that the movements were still going on. This search gave the first evidence of an endogenous rhythm lacking visible indications and De Candolle lately confirmed this observation in 1828 who also observed the leaf movements in many other plants (2).

Wilhelm Pfeffer in 1875 studied sleep movements in *Acacia lophantha* and confirmed the resumption of rhythms in plants which have been kept in constant light or dark. This observation additionally grabbed the eye of Charles Darwin, which resulted in observing the movements in over 300 plants and ultimately "The Power of Movement in Plants" in 1881. The idea of the inherited nature of movements got further support by experiments done by Semon in 1905 (2).

Carl Linnaeus likewise watched time-subordinate conduct in plants. In 1751, he distributed a greenery enclosure plan for a bloom clock, demonstrating the time by utilizing plant species that opened and closed their blossoms at various occasions of the day (3).

Figure 1-1. Linnaeus Flower Clock

A garden clock consisting of different flowers which open and close at different times of the day. Floral Clock, Victoria Square, Christchurch. Photo by Greg O'Beirne, 2004

Erwin Bünning, the German plant physiologist, established the genetic characteristic of circadian rhythm by demonstrating this in bean plants. He considered circadian rhythms as inherent property in plants and suggested that rhythms are adaptive. Bünning stressed the dependence of clock on the physical rather biochemical mechanism and presented that light rather than any cosmic factor-regulated movements in plants. Sunlight is essential input acting through photoreceptor to entrain the clock to local time. His work is deemed to mark the beginning of photoperiod research on plants (2).

However, the foundation of modern chronobiology is usually attributed to the two scientists Colin Pittendrigh and Jürgen Aschoff, who started to study this field in the 1950s. They developed much of the nomenclature that is still used in clock research, using a variety of models from flies to finches to humans.

1.2 Properties of Circadian Rhythm

Free running conditions need to exist for a rhythm to be considered as circadian and differentiated from other rhythms. A circadian rhythm persists with a periodicity of about 24 h in the absence of all-time signs, i.e. in constant conditions. In response to transitions between light and dark, high and low temperatures or metabolic signals, it must also be trainable. Moreover, it should be cradled against ecological 'clamour, for example, stochastic variation in light and temperature, consequently just reacting to changes in the condition that should be in synchrony with the encompassing day-night cycle. As a feature of this system, the circadian

clock is most receptive to light around sunset and daybreak, while it is least around the center of the day/night.

For simplification, the circadian clock can be partitioned into three sections, as delineated below: Input pathways that transmit signals, for example, light and temperature, from the earth to the Central oscillator, which works as a negative feedback loop figuring out the outcome of signals (figure 1-1) resulting in the signal diverted to output pathway generating overt rhythms (4-6). Recent research put attention on the existence of several interconnected feedback loops having different components affected by light and temperature.

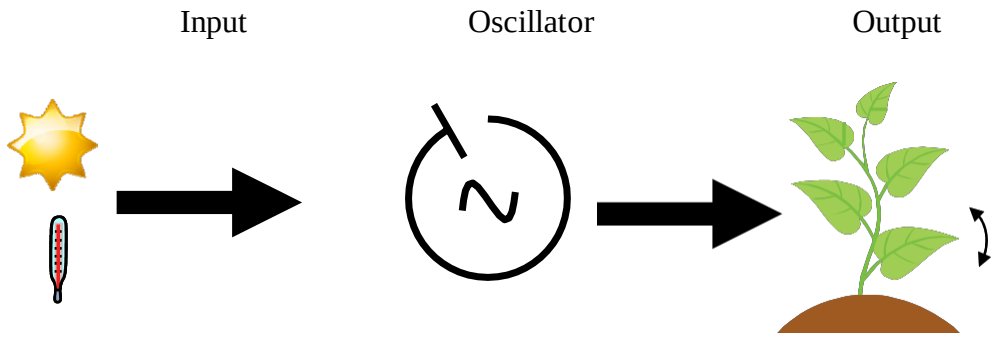

Figure 1-2. Function of a circadian oscillator.

The response of clock to a stimulus, for example, is regulated by the circadian clock and the expression of the specific gene varies over the circadian cycle (7-9). This implies the clock is responsive only at certain times of the circadian cycle while at other occasions the gate for light input is kept closed. Such a distinction allows differentiating between the immediate and gated response to a stimulus.

The procedure by which the biological clock re-sets itself following natural signals is called entrainment. The most evident signals for entrainment are the everyday changes among light and dark, even though shifts among low and high temperatures are likewise essential and adequate to entrain clock-controlled rhythms.

Light intensity is another factor that influences a circadian rhythm period. Jürgen Aschoff found an inverse linear relationship between the irradiance and the length of the period. Diurnal organisms kept at a high light intensity will have shorter free-running times compared to counterparts kept under lower light intensities, whereas the opposite is exact for nocturnal organisms. This conduct of the clock is otherwise called parametric entrainment and this specific marvel is alluded to as ' Aschoff's rule'. To explain entrainment, two theories seem to be relevant in this regard. Aschoff's continuous or parametric entrainment theory considers that

the clock is affected by light during the whole circadian cycle (10). Effect of light intensity on the period is taken as evidence for this model (Aschoff's rule). Pittendrigh's discrete theory, in contradiction to continuous entrainment theory, presents the view that the clock is reset instantly by sharp changes in light intensity as at dusk and dawn, thus enhancing adjustability with an environment (11). This model better explains entrainment in Drosophila and rodents. The term Zeitgeber is used for environmental stimuli which can reset the clock. Variation in light pulses, as well as temperature fluctuations, can be termed as zeitgebers for plants (11). However, the possibility of presence combined mechanisms responsible for entrainment was also presented by Aschoff (12).

The clock has a point of singularity, which is the point where the clock begins again. Before this point, if light pulses are given, the phase will be delayed, while after this point, if light pulses are given, the phase will progress. This point usually occurs in a 12 h light/12 h dark cycle in the middle of the subjective night (11, 13).

There is also a "dead" zone in which, in the middle of the day, light signals do not affect the phase. Thus, by building such a PRC, it is possible to predict when the light should be applied to achieve stable entry, providing information about the behavior of the clocks in the organism being examined.

There are specific essential terms related to circadian rhythms, which are summarized in the following Figure 1-3.

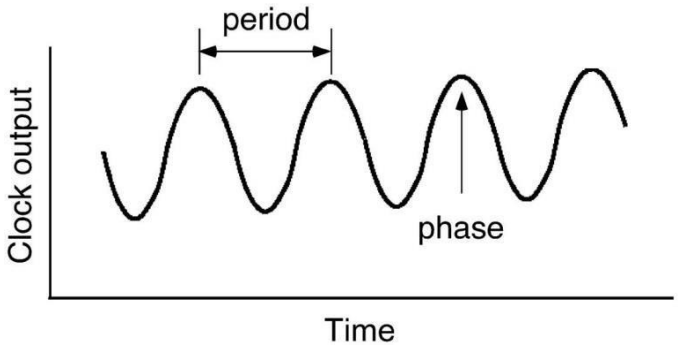

Figure 1-3. A circadian oscillation. The time used to complete one cycle, is called the" period". The period is usually measured from peak to peak. The time of day for a given event, is defined as the" phase" (20). The output of the clock may be movements, growth etc.

1.3 Circadian cycle and homeostasis

The phenomenon of matching internal and external rhythms is called ' resonance ' and is also essential for plants as it has been shown that plants with an internal clock period corresponding to the surrounding environment grow much better and accumulate more starch than plants with an inappropriate internal clock period (14).

The ability to maintain this stability among the functions of different organs was named homeostasis, the term coined by Harvard physiologist, Walter Cannon combining two ancient Greek words after extending the concept of (milieu interne) presented by Claude Bernard.

Management of constant internal environment is required for the various process running in organisms ranging from maintaining electrolytes, securing enough energy, and ensuring hormonal levels for growth and reproduction. The reason for maintaining this balance is debated as to whether its intrinsic property of organism to behave such a way against external stress or this is part of learning.

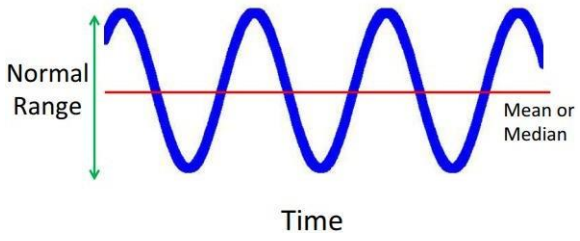

Figure 1-4. A graphic depiction of the principle of homeostasis. Any biological function or measurement will oscillate around a mean or median within a range that is considered a normal or physiological.

Walter Cannon wrote in Wisdom of the Body (15) *"The word does not mean something set and immobile, a stagnation. It means a condition-a condition which may vary, but which is relatively constant."* (16). According to Arthur C. Guyton maintenance of nearly constant conditions in the interval, the environment is considered homeostasis by physiologists (17). Stress can be of different kind and nature as extreme temperature fluctuations, food deprivation, oxidative or hypoxic stress, emotional and psychological, to name the few. As homeostasis is maintaining internal conditions within normal range but not keeping them constant, Kelvin J.A. Davies proposed the term Adaptive Homoeostasis defined as transient expansion or contraction of homoeostatic range in response to sub-toxic, non-damaging, signaling molecules or events, or removal or cessation of such molecules or events (18).

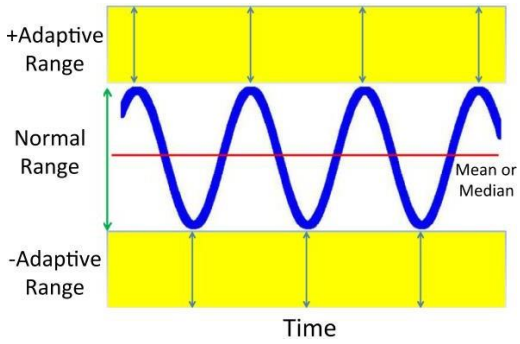

Figure 1-5. A graphical representation of adaptive homeostasis (137).

Hence to keep the conditions in homoeostatic range, it seems necessary to exist counterpart systems to control both upper and lower borders. Nevertheless, positive and negative feedback control systems are essential for physiological functioning or simply homeostasis in a living organism. Ovulation stimulated by gonadotropins as well as the release of oxytocin during parturition induced by fetal head pressure on the uterine cervix are examples of positive feedback.

Positive feedback is far less frequent for the logical reason that, if uncontrolled, may cause self-destruction while negative feedback controls comprise of a system in which the moderate output strength of the controllers to a predetermined setpoint level. The setpoint is not fixed value; instead, it is adjustable depending on relationship inflow and outflow controllers. The setpoint is illustrated as a defined value of engineering devices, yet it can be misleading in physiological systems. In physiological models set point acts as a threshold to generate motivated behavior in a coordinated manner to protect the regulated variable against homeostatic challenge. Different from the controlled engineering thermostat, the set point in living organisms cannot be the same in changing conditions (19). Its variable yet defined defendable range may vary according to multiple factors. Nevertheless, the deviation from the setpoint is to such an extent that the change is felt, and effector mechanisms are put to work to oppose further deviation of the regulated variable. Such a defensive strategy to protect from the extreme conditions was thought to be done by inter-related negative feedback loops.

So, what are the mechanisms on which homeostasis and circadian rhythms based on? Homeostatic processes are found to contain negative and positive feedback loops. Negative feedback is a form of communication which works in contrary to what the program already does (19). In the mammalian liver, at least two bile acid biosynthesis pathways were described. These pathways are separately controlled, but negative feedback is a core component of both controls (20). In this loop, higher concentrations of bile acid leads to lower

expression of CYP7A, CYP7B and CYP8B, resulting in reduced synthesis of bile acid (21). The hypothalamus – hypophyseal – adrenal system (HPA) is closely linked to stress and homeostasis restoration, it is centered on three basic rules that comprise a homeostasis principle and unlike other models, its main elements include a positive feedback loop in addition to the traditional negative feedback component (22).

The demand for nutrients follows a rhythmic pattern as a result of diel changes in photosynthesis and transpiration rates, for example, suggesting that they are under close metabolic and clock control (23). Cytosolic free Ca concentration is rhythmic (24) and most likely under circadian clock control (25), providing the biological oscillator with a potential mechanism for modulating some of its outputs. In addition, transcripts of genes coding for multiple channels and Ca-related transporters have been shown to be clock-regulated (23, 26).

Similarly, for the generation of circadian rhythms, both positive and negative feedback loops of transcriptional regulation have been suggested and the sufficiency of the proposed mechanisms has been determined in *Neurospora crassa* and *Drosophila melanogaster* circadian oscillators. Hence, in *Arabidopsis thaliana*, the proposed model of circadian clock describes an input pathway by which photo perception takes place and light signals are translated into environmental signals for a circadian oscillator ; (the circadian oscillator generating rhythm) ; and finally, there are output mechanisms through which the temporal signals produced by the oscillator control cellular behavior (27).

1.4 Model organisms for clock study

Great discoveries have been made by scientific communities using model organisms for other similar species. Usually, a relatively simple organism is selected to be used in experimentation, yet the findings can be applied to explain systems in more complex organisms. Such organisms have also been beneficial in explaining the genetics behind the circadian clock.

1.4.1 Neurospora crassa

The primary eukaryote *Neurospora crassa* has been utilized in circadian research for more than 50 years (28, 29). The genes that are at the heart of the Neurospora clock include *FRQ*, *FRH*, *WC-1*, and *WC-2*, of which *WC-1* and *WC-2* function as positive elements in a feedback loop, while *FRQ* and *FRH* are negative. *FRQ* expression is also regulated by temperature and different forms of the FRQ protein are produced depending on the temperature that regulates transcript splicing (30).

1.4.2 Drosophila melanogaster

Drosophila melanogaster has been one of the organisms got attention for clock studies. Adult emergence (eclosion) and locomotor activity are examples of circadian outcomes (31). Colin Pittendrigh did study on eclosion in 1954 and described the rhythms were seen to be under control of biological clock (32). Ron Konopka and Seymour Benzer discovered the first clock mutant in *Drosophila melanogaster* (33). They called it *per* gene and lately it was found that per locus has basic role in biological clock (34).

Three genes are central to the current scientific understanding of clock pathways: The Clock (Clk) transcription factor and the Period (Per) and Timeless (Tim) transcription repressors. The Drosophila clock comprises two loops of feedback, one involving the genes *per* and *tim* and the other the gene *clk*. Additionally, the fine tuning of the clock involves some other genes.

1.4.3 Gonyaulax polyedra

Njus et al. (1977) discovered that circadian light rhythms in the *Gonyaulax polyedra* algae vanished when its outer temperature dropped from 20 to 12℃ but remerged, with a phase correlated with the time of transition when the temperature returned to 20℃ (35). The bright light can also similarly induce periodicity loss and restarted by darkening the environment of the organism. Thus, there has been synergy in *Gonyaulax polyedra* between the light and temperature cues.

1.4.4 Arabidopsis thaliana

In *Arabidopsis thaliana*, common name Thale Cress, the role of the circadian clock is studied most extensively. Only due to its compact, fully sequenced genome and relatively fast life cycle (seed to seed in about six to eight weeks), this plant is the subject of most basic plant molecular research, among other beneficial features.

The circadian clock in *Arabidopsis* plants regulates several biological processes, such as rhythmic leaf movement (36, 37), petal opening (37), the elongation rate of stems, hypocotyls and roots (38-41) circumnutating of stems (42).

1.5 *Arabidopsis thaliana* clock

TIMING OF CAB EXPRESSION1 (TOC1) the gene expressed at evening was the first clock gene to be found in *Arabidopsis thaliana* (5)**.** CIRCADIAN CLOCK ASSOCIATED1 (CCA1) (43) and LATE ELONGATED HYPOCOTYL (LHY) (44) are two single MYB domain

transcription factor genes with the highest expression of both transcripts and proteins around dawn (45).

The inner feedback loop is assumed to be comprised of the above described three genes, where the expression of CCA1 and LHY genes is promoted by TOC1 protein during the night. On the other hand, CCA1 and LHY proteins, in turn, repress TOC1 gene expression during the day (46-48). When the levels of TOC1 decrease, the promotion of CCA1 and LHY transcription decreases, allowing TOC1 levels to increase and promote CCA1 and LHY transcription again. All this takes place in a cycle of about 24 hours, as shown in figure 2-2. Later this was found that the circadian model for *Arabidopsis thaliana* is not so simple.

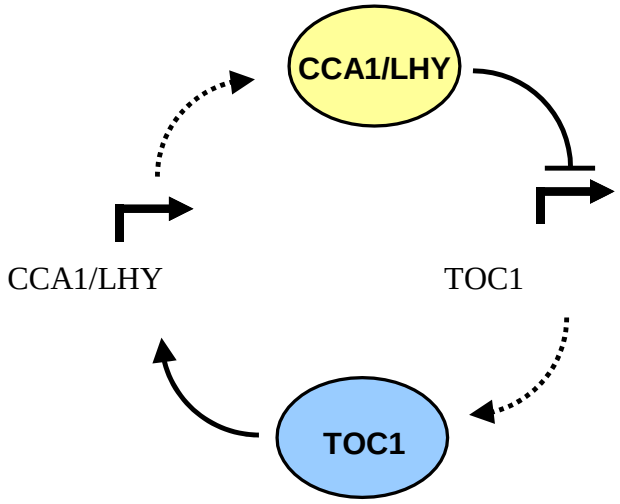

Figure 1-6. The genes and proteins making up the circadian core oscillators. TOC1 promotes expression of CCA1 and LHY, which in turn represses transcription of TOC1. This leads to a decrease in TOC1 protein levels and thus a decrease in CCA1 and LHY. This allows TOC1 transcription to increase again and TOC1 protein can once more promote CCA1 and LHY. All this happens over a ~24h cycle (49).

1.5.1 History of the Plant clock

In plants, molecular - level research accelerated by Steve Kay and Andrew Millar as they introduced the firefly reporter gene LUCIFERASE (LUC), fused with the photosynthesis gene CHLOROPHYLL A / B BINDING PROTEIN 2 (CAB2*)* (3, 50) Into the Arabidopsis thaliana model plant. The expression of CAB2 is controlled by both the circadian clock and phytochrome (phy) photoreceptors (3, 51).

Photosynthesis is essential for plant growth and many circadian rhythms of plants are linked to photosynthesis (52). The possible role of the clock in the process of light harvesting is to anticipate the period of light, allowing the plant to prepare for photosynthesis. This maximizes energy consumption throughout the day by running the photosynthetic machinery from first light. The circadian clock is therefore essential in directing metabolic and developmental events to the most favorable time of the day, maximizing the growth of the organism and its chance of survival.

1.5.2 Photoperiodism

The length of duration of light in a day is termed photoperiod while the effects on organism due to this light are known as photoperiodism. Among the biologists, Bünning was first to propose the control of diurnal rhythms on reproductive responses (53). Based on the sections of the day expected to light or dark, he separated two phases of a day, i.e., photophil and scotophil phase. Following this idea, responses for a short day could be observed if the rhythm was confined to the photophil phase, while long day responses were possibly seen as rhythm continues into the scotophil phase.

Colin Pittendrigh later considered two comparative models, the outside and inner coincidence models (54). The response will generate if the rhythm will be in phase with external light stimuli, according to the external coincidence model. The model of internal coincidence was based on the theory that an organism has several independent oscillators linked either to dawn or dusk.

The seasonal changes such as flowering, is among several effects of photoperiods. As springs proceeds, the days start becoming longer than nights. Hence flowering accelerates in long day model plants like *Arabidopsis thaliana*. While tobacco, a short-day species, will flower only

under short days. The flowering in tobacco plant was controlled by daylength was discovered by Garner and Allard in 1920 (55). To study these transient changes effectively, the clock needs to run precisely and not be delicate to arbitrary, momentary ecological fluctuations.

1.5.3 Phytochromes

In contrast to animals, plants have photoreceptors in every cell. The light perceiving pathways in *Arabidopsis thaliana* has been under extensive study. Among other functions, light has an entrainment effect on plant clock. There are several types of photoreceptors(phytochromes) in plants having the sensitivity to different light wavelengths. Red and far-red light perception are done by the phytochromes (phyA-E) (56). After getting activated by red light, these become inactivated if further exposed to far-red light. A natural equilibrium exists between activated and inactivated conditions of phytochromes depending on the red/far-red ratio. PhyA, with its specific features, acts as a highly sensitive light antenna. PhyA, B, D and E are considered to influence the clock, presumably by influencing the perception of photon irradiance (5, 6).

Circadian period decreases with increased light intensity (5) whereas it increases with longer photoperiods during entrainment (57). Light input to the system is provided by the phytochromes, acting through PHYTOCHROME INTERACTING (PIF) proteins (58), cryptochromes and ZTL (59). Increments in irradiance lead to shortening of yield of leaf development and in gene expression periods in *Arabidopsis thaliana* (5, 36, 60) . Importance of phytochromes in resetting the clock is also accepted (61, 62). Blue light receptors are the cryptochromes (cry1 - 2). By the action of blue light, they are phosphorylated and thus become biologically active (63). Cryptochromes affect clock inputs and flowering pathways via the E3 ubiquitin ligase COP1 (64). The *pry* and *cry* gene families thus focus on circadian guideline at the transcriptional level, albeit circadian control at the protein level is of low extent (65). Phototropins has an essential role in the perception of blue light hence in stomata opening and chloroplast movement. These proteins have LOV domains, a common feature with ZEITLUPE (ZTL) (62). The involvement of ZTL degrades TOC1 and PRR (66, 67). TOC1, which also interacts in stabilizing way with GIGANTEA (GI) (68).

1.6 Mathematical modelling approach

The level of genes involved in the clock is regulated by translational and post-translational complex feedback loops, which make it difficult to understand the behavior of the system to perturbations without using mathematical modelling. Modelling generates insight into genetic interconnections together with experimentation. Mathematical models permit a detailed study of complicated gene network complexities and architecture (69-72). In the past, simulations of circadian oscillators capable of reproducing essential qualities of the quantitatively studied rhythms were characterized for different organisms (Neurospora (73, 74); mammals (75, 76); Drosophila (77, 78). Models were initially formed with mechanisms that account with a minimum number of components for the desired clock attributes. However, it is essential to provide many new components that will be discovered later in the next modelling step in these first - generation oscillators. The use of optimization techniques to calculate variables that best account for a selection of clock attributes a vital contribution to the experimental work. Constant experimentation iteration is necessary and plays a significant role in the scientific validity of mathematical models. Another task that modelers face in estimating parameters. There is not always a straight interaction between single parameters and a biochemical process, and the quantification of reaction rates is either noisy or impossible. Clocks are shown to be entrained by 24-hour input increments and phase receptive to 24-hour oscillations. The phase is modified by single external stimuli, depending on the current interference phase. The only model input for the clock so far in plants is light, though the inclusion of temperature influence can be useful for further modelling of the circadian plant system.

1.7 Molecular model for clock

The clocks are made up of a network of transcription factors arranged in interlocking negative feedback loops (79). Furthermore, the circadian rhythm elements between the kingdoms are not conserved. This indicates that on several occasions' clocks may have evolved independently (80).

The circadian clock is divided into three components: the "input" pathways to receive and communicate the stimuli to a central oscillator which generates the rhythmic outcomes such as

flowering or leaf movement while "output" pathway links this oscillator to determined biological processes. Generally, the inputs are light or temperature, which harmonizes the central oscillator with an external environment.

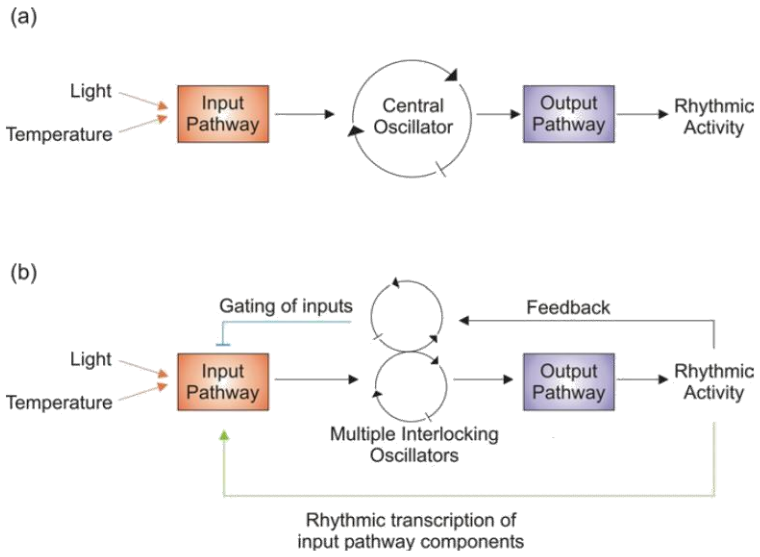

Figure 1-7. Simple representations of circadian clock model (a) Light information is perceived by a photoreceptor that passes the information to the central oscillator, entraining it to the correct time of day. This core oscillator, via the output pathway controls the observable rhythms (79) (b) A more detailed clock model containing multiple core oscillators and gated input pathways and outputs which feeds back to the central oscillator. Figure from (79).

However, in explaining the circadian clock's intricate network, these simple clock systems are not solely enough. That is because several components of the input pathways are clock outputs themselves, and rhythmic outputs from the clock can feedback to affect the core oscillator's functioning (79). Moreover, multiple interlocking loops compose the core oscillator in *Neurospora crassa*, *Drosophila melanogaster*, *Arabidopsis thaliana* as well as mammals (81, 82).

In *Arabidopsis thaliana*, mutant screening and genetic mapping - cloning approaches were conducted to obtain an essential understanding of the molecular mechanisms behind the plant clock. This culminated in the identification of at least 25 clock function - affiliated genes (83). It became evident that these genes interact to arrange a "genetic circuit" underlying the endogenous period of 24 hours (83).

1.8 Models of the Arabidopsis thaliana clock

1.8.1 LHY / CCA1–TOC1 Model

This model demonstrates that the clock's basic feedback system, but the full interface of the clock is too simple to be represented in this way. The regulation of the clock requires several other molecules, forming several interrelated loops (84). Several other clock genes have been found in *Arabidopsis thaliana*, reviewed in (85-87), but either have accessory functions (88) have not yet been located in direct relation to the LHY / CCA1–TOC1 single-loop model.

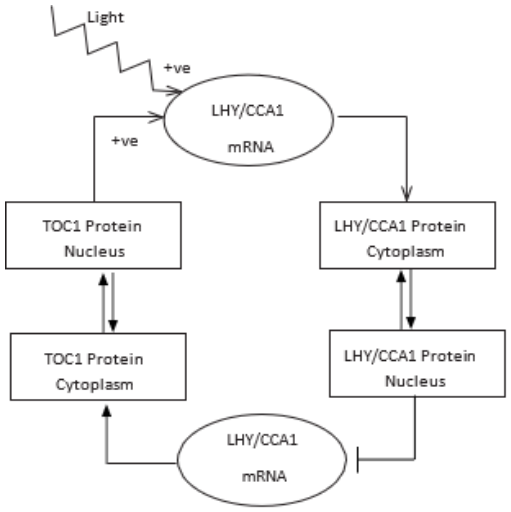

Figure 1-8. Model for the central feedback loop in the Arabidopsis clock. TOC1 proteins in the nucleus and light, mediated by protein P (not shown) positively activates transcription of LHY and CCA1 mRNA. When LHY and CCA1 proteins reach the nucleus they down regulate TOC1 mRNA transcription (84).

Mathematical modelling based on experimental and theoretical data is useful to understand how this complicated system is configured (84, 89, 90). Locke et al. hence introduced modelling of the Arabidopsis clock by examining the one-loop LHY/CCA1–TOC1 model, using a scheme that will be widely applicable in trying more extensive genetic networks. By evaluation with experimental data, the model predicts where additional component(s) of the clock network may function (84, 91).

Using the single - loop LHY / CCA1– TOC1 network showed that the phases of wild type TOC1 and LHY RNA accumulation under the light-dark cycle (LD) 12:12 could be reproduced correctly by this network (91). Simulated concentrations of TOC1 RNA remained high until LHY protein accumulated rather than falling as asserted after dusk. There must, therefore, be another significant factor responsible for reducing the expression of TOC1 that this network does not have.

The TOC1 fusion was shown to have lowest abundance close to dawn under LD12:12, whereas according to the LHY / CCA1–TOC1 single - loop network, TOC1 should activate LHY transcription at that time to the maximum (84). This suggests that either the active TOC1 form is present at a much lower concentration than the bulk TOC1 protein, possibly in a complex, or that the direct activator of LHY and CCA1 is an additional TOC1-dependent component (91).

The third problem is that the LHY / CCA1–TOC1 network has failed to respond to the daylight, while experimentally it is apparent that the clock has a later phase under longer photoperiods (7, 92). This restriction occurs because light input to this network is only modelled by triggering LHY expression at dawn, so at the end of the photoperiod the model is insensitive to light. Indeed, and CCA1 expression drops to a low level before the end of a 12-hour photoperiod (45) hence close to night, another mechanism is needed to mediate light input.

1.8.2 LHY/CCA1–TOC1-X Model

The model was expanded the LHY / CCA1–TOC1 single - loop network by introducing components as aimed by the experimental data to address these constraints.

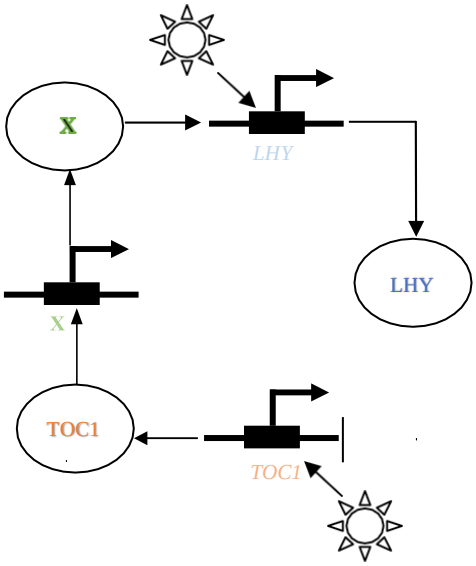

Figure 1-9. The single-loop LHY/CCA1–TOC1-X network. LHY and CCA1 are modelled as a single gene, LHY (genes are boxed). Nuclear and cytoplasmic protein levels are grouped for clarity (shown encircled) and degradation is not shown. Light acutely activates LHY transcription at dawn and activates TOC1 transcription throughout the day. TOC1 activates a putative gene X, which in turn activates LHY. Nuclear LHY protein represses TOC1 transcription (89).

First, light activation of TOC1 transcription was included in order to provide light input at the end of the day and, conversely, to reduce the activation of TOC1 immediately after lights - off. Second, after TOC1, an additional gene X was added to the network, with nuclear X protein being the immediate LHY activator instead of nuclear TOC1. Thirdly, since the F - box protein ZEITLUPE (ZTL) was shown to degrade TOC1 protein more effectively at night (93).

By making these modifications, it was observed that TOC1 levels of RNA peak in Arabidopsis at dusk below LD12:12, and dawn LHY levels of RNA. As observed in the experiment, the model allows TOC1 mRNA levels to drop before LHY levels rise. Including gene X in the model, TOC1 protein levels can be simulated to fit well with published data. It is also possible to predict X mRNA and protein levels. X mRNA peaks under LD12:12 in the middle of the night and nuclear X protein peaks at dawn (84, 91). Furthermore, this model still fails to predict a long period in the simulated cca1 single mutant and the strong, LL activation of TOC1 transcription causes several problems, e.g. the model becomes arrhythmic with long photoperiods under LD cycles.

1.8.3 The interlocked feedback loop network

Deleting LHY component from single - loop models discourages any oscillation (data not shown), so none of these designs can reproduce the adaptable, accentuated rhythms observed in cca1; lhy plants. Therefore, a network of interconnected feedback loops was formed capable of oscillating in simulated cca1; lhy double mutants. A hypothetical gene Y activates transcription of TOC1, and the protein TOC1 suppresses transcription of Y, forming a loop of feedback. The suggestion that TOC1 has both a negative and a positive function is novel. Light input into this loop occurs through Y rather than TOC1 transcriptional activation (94). Y is repressed by LHY. Therefore, LHY acts as a powerful early - day delaying factor in inhibiting both TOC1 and Y expression (91).

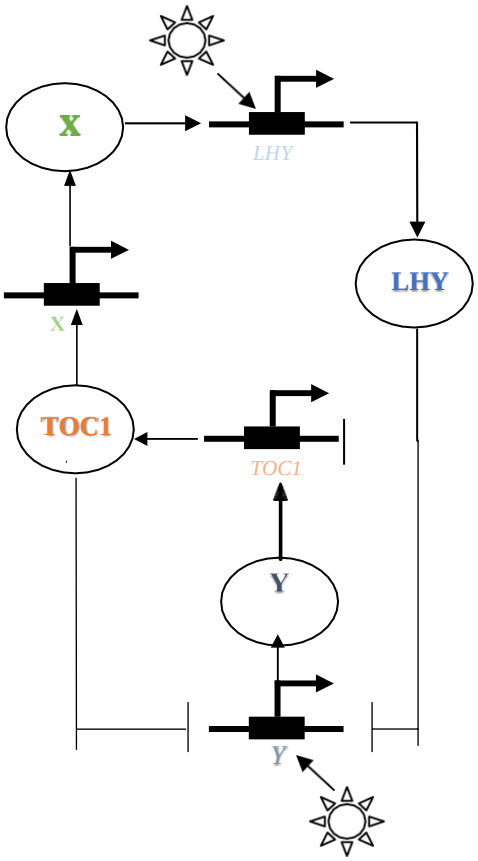

Figure 1-10. The interlocked feedback loop network: Compared to Figure 2-4, TOC1 is activated by light indirectly via hypothetical gene Y. Y activates TOC1 transcription and both LHY and TOC1 repress Y transcription, forming a second feedback loop (91).

The model with the optimal parameters of the interlocked feedback loop fits with the data (not shown), and its behavior is also robust to change the parameter. Some parameters have more sensitivity to change than others in preceding clock models (78). This model's time and amplitude are far less sensitive to changes in parameters than the LHY / CCA1–TOC1 single-loop model, implying that some of the single - loop model's shortcomings have been alleviated (91). This is the first model to fit well with LL data for mRNA levels of LHY and TOC1. The optimal set of parameters minimized light regulation of the degradation of TOC1 indicating that light - regulated degradation (66) is not necessary to be adjusted by these data. Simulation of ztl mutants by halving the total degradation rate of TOC1 results in a phenotype of 28 hours, again similar to that found in ztl mutants (91).

As anticipated, the interlocked feedback model's trained phase is photoperiod responsive with simulated levels of mRNA peaking later as observed under longer photoperiods (92, 95). Light input to Y enables the network throughout the day to respond to light. Therefore, this network will be a good starting point for the photoperiod sensor models involved in flowering time (91). The entrainment range of the photoperiod is approximately 3:16 h light for a 24-hour timeframe

and the simulations remain trained for an approximate range of 22–30 hours, where half of the time is light and half dark. At the end of the ranges, the entrainment produces a beat in amplitude, although with little phase effect. To measure the impact of their contribution on entrainment of the circadian clock, the balance of light input to LHY, Y and ZTL should now be examined in more detail (91).

1.8.3.1 Understanding of interlocked two loop model

The final, interlocking loop model represents a more significant data range than the single loop models, including the entrain able short - term oscillations. Two putative genes X and Y were included in the development of this model and used experiments designed from model predictions to identify GI as a Y candidate gene. The interlocked feedback model now emphasizes the importance of GI as an element of light input to the clock, a role that was not previously highlighted and should now be tested in more detail. GI's activation of TOC1 in an interlocked feedback loop is also a new proposal, consistent with the peak GI expression timing before TOC1. A recent study indicated that a feedback loop between APRR9/APRR7 and LHY / CCA1 appear to exist (96). The importance of light input pathways in these models was to be expected because it is known that the circadian plant system interacts in a sophisticated way with multiple photoreceptor pathways (93, 97). For example, tracking multiple phases during entrainment requires at least two light inputs to two feedback loops (98) present in our final model. The Arabidopsis clock's entrainment trends under various photoperiods (7) show that the clock phase does not merely track the dawn. Thus, at times, other than the dark - light transition, the clock must obtain light inputs. LHY enables light input at dawn in our model, while the input to Y and ZTL is possibly useful all day long.

Repression of Y by LHY and TOC1 is adequate in the interlocked loop model to gate the light activation of Y, so we had no rationale for additional modifications to this model. Such models should be viewed with caution as it is not possible to expressly include unexplored components as the model that concisely summarizes the regulation of known components is probable to have captured the pertinent effects of the concealed components (89, 91). Anyhow, the models will help us to understand how circadian output mechanisms enable the clock's few genes to control a thousand rhythmically controlled genes in the genome of *Arabidopsis thaliana* (99).

1.8.4 Three loop model

The interconnected two-loop model predicted two hypothetical components X and Y's existence and expression patterns. X is suggested to activate TOC1, and X protein activates LHY transcription as required by the TOC1 protein expression profile (90, 91, 100). Y forms a second loop with TOC1, responsible for the lhy; cca1 mutant's short - term oscillation. GI has been recognized as a candidate for Y based on the resemblance of expected and observed patterns of expression (91). In the following figure, the model was extended to include the newly proposed feedback loop between PSEUDO-RESPONSE REGULATOR 7 (PRR7), PRR9 and LHY / CCA1 (13, 96), resulting in a three-loop circuit figure 2-6.

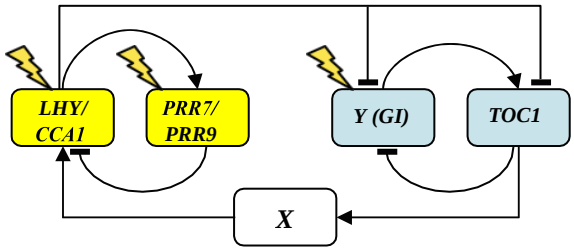

Figure 1-11. The Arabidopsis clock model with three loops represents 20 h rhythms in toc1 mutants. 3-loop network summary, showing only genes (boxed), regulatory interactions (arrows) and light input locations (flashes). Two - component oscillators are characterized by yellow or blue shading of gene names(96).

A possible method to account for this oscillation was provided by the proposed PRR7/PRR9–LHY / CCA1 feedback loop. To create a three-loop model, we added this loop to the interlocked feedback model. Since PRR7 and nine mutant phenotypes are weak, apparently less than one h different than WT (101) these genes were grouped as one gene, PRR7/9. LHY and CCA1 have been grouped as LHY (91). The first feedback loop involves the activation of PRR7/9 transcription by LHY (96) with the repression of LHY activation by PRR7/9 protein. Our previous model presents the rest of the network (91). LHY suppresses TOC1 and Y transcription; LHY has experimental support for the dual, repressive, and activating role (96). X transcription is activated by the TOC1 protein, with X activating LHY transcription to form a second feedback loop. Y activates the expression of TOC1 and TOC1 represses Y expression, creating the third loop of feedback. Analysis of sensitivity demonstrates that the three-loop model is tolerant of variable changes comparable to the interlocking - loop model.

1.8.4.1 Outcomes from the three-loop model

The model predicts that two short - term oscillators, the morning - expressed PRR7/9–LHY / CCA1 loop and the night - expressed TOC1–Y / GI loop, will be combined with the LHY / CCA1–TOC1–X loop. At a fixed phase relative to dawn, the clock - controlled expression of

LHY mRNA before dawn (20–24h) remains. By contrast, under long photoperiod conditions, the peak of TOC1 mRNA is delayed, showing that its phase also reacts to dusk time. This leverage is not seen in one - loop or interlocked - loop models, where clock - controlled expressions of LHY and TOC1 are fixed relative to dawn, or either move with dusk. The clock's three-loop structure allows flexibility in tracking multiple phases (98). Also, the three - loop model shows that if the coupling between the PRR7/9–LHY / CCA1 loop and the TOC1–Y / GI loop expressed in the evening were impaired, the two oscillators could run within one cell with different periods. It is not yet complete as it does not include known clock - affecting genes such as PRR3, PRR5, TIME FOR COFFEE (TIC), EARLY FLOWERING 4 (ELF4) and LUX ARRHYTHMO (LUX). The three - loop circuit adds to the apparent effectiveness of the Arabidopsis clock, together with the partial inefficiency of specific genes: few single mutations change the clock period by more than 3–4 h and arrhythmic mutations are uncommon (102). The three - loop model is more realistic because it can induce the short - period rhythms and the long - period rhythms while still correctly matching the previous model's mutant phenotype. Modelling provides a vital tool for targeting future mutant redevelopment and retrieving the maximum value from time series studies using existing local genetic resources.

The three - loop model provides a framework for such intracellular desynchronization if different loops influence the vastly different rhythmic mechanisms and under certain situations, the coupling between loops is weakened. This flexibility of circadian regulation is expected to give a selective advantage, especially when seasonal changes in the photoperiod fluctuate the relative dawn and dusk timing. Plant clocks are only weakly paired between cells, if at all (103) but the three - loop circuit implies that an comparable design can be built within a single cell by modulating the morning - expressed gene loop LHY / CCA1 and PPR7/9 to the night - expressed TOC1–GI loop. Yet it will be important to recognize the role and balance of light inputs for each of the clock's feedback loops, first to ascertain what flexibility the three - loop circuit can provide and then understanding the evolution in plant take advantage of this flexibility in regulating rhythmic processes at varying times of the day.

1.9 Summary of the literature

Mathematical modelling based on experimental and theoretical data helped understand how this complex system is configured (84, 89, 90). At least three interconnected feedback

mechanisms make up the clock in the most current but inconclusive theoretical model of the clock, and two unknown factors X and Y are anticipated to be significant players. Most likely, these factors include the action of many undetermined genes. These loops are then further co-ordinated by additional interactor(s), e.g. EARLY FLOWERING 4 (ELF4) (104). TOC1 belongs to the PSEUDO-RESPONSE REGULATORS gene family. It includes five genes: TOC1 (PRR1) and PRR3, PRR5, PRR7 and PRR9 (85, 105, 106). Though their single mutant phenotypes are overt, all these genes play a significant role in the clock (101, 105-107). During the diurnal cycle, they all oscillate with various peak times (107-111).

PRR7 and 9 form a second CCA1 and LHY feedback loop (96), acting in the morning when CCA1 and LHY promote them. In turn, they repress CCA1 and LHY transcript expression; PRR7 and PRR9 proteins have recently been shown to attach CCA1 and LHY promoters in a repressive fashion along with PRR5 protein (112). It has been shown that PRR5 interacts with and is degraded by ZTL through interaction between ZTL's light - oxygen (LOV) domain and PRR5 domain (113). PRR5 is also biologically related to GIGANTEA (GI) and acts on the flowering regulator CDF1 (114) to regulate photoperiodic flowering time. ZTL is an F - box protein that forms part of an E3 ubiquitin ligase complex of Skp / Cullin / F - box (SCF) (115-117). The protein structure also comprises a LOV / PAS domain that allows blue light to be sensed. It interacts with both TOC1 and PRR5 via its LOV domain, leading through the proteasome pathway to their degradation (66, 113). ZTL works in conjunction with GI through the LOV domain, which cyclically stabilizes the ZTL protein (113). GI also interacts with the FKF1 ZTL counterpart depending on the blue light action (118). Although the levels of ZTL mRNA appear constitutive, the levels of ZTL protein oscillate (68). All ZTL protein-protein relationships are involved in demonstrating the significance of ZTL and other subsystems post-translation regulation of clock components (119, 120).

PRR3 tends to increase TOC1 by hampering TOC1 degeneration reliant on ZTL (121). The GI gene demonstrated in the evening is engaged in both clock regulation and floral regulation (122, 123). At least part of the expected factor Y in the clock model was also suggested (89).

To combine all these pieces of information, mathematical modelling indicates that the clock consists of at least three feedback loops : a core loop consisting of CCA and LHY and TOC1, in which TOC1 acts through factor X on CCA1 and LHY, a morning loop composed of CCA1 and LHY and PRR5/9, and an evening loop with TOC1 and the unknown factor Y, at least partly comprised of GI. Lately, it has been shown that CCA1 HIKING EXPEDITION (CHE)

binds the promoter of CCA1, represses its behavior, possibly by intervening with TOC1 activity (124), moreover, may be part of factor X predicted. The fact that roles of these proteins have not yet been fully defined shows that knowledge of the clock system in Arabidopsis, and plants in general, is inconclusive and it is relatively likely that additional proteins will be discovered that are engaged in these biological processes.

1.9.1 Further findings on the *Arabidopsis thaliana* clock

While originally considered as linear entities, increasing evidence suggests that many signaling pathways within the overall network can act as both inputs and outputs for one another as can be seen in Figure 1-12. Two additional phase - specific feedback loops were proposed based on experimental observations and mathematical modelling (89, 90). One such circuit is a morning loop where CCA1 and LHY directly activate the expression of two TOC1 homologues, PSEUDORESPONSE REGULATOR 7 and 9 (PRR7 and PRR9). PRR7 and PRR9, in turn, are partially redundant to inhibit CCA1 and LHY expression. Although the process underlying this control is not transparent, extrapolating the relationship between CHE and TOC1 suggests that PRR7 and PRR9 may interact with CCA1 or LHY promoters related transcription factors. The other feedback loop involves the induction of TOC1 by an unknown (generally called Y) component or function of the evening clock. Y was also predicted in this evening loop to be light-inducible and negatively controlled by TOC1, CCA1 and LHY (91). A protein called GIGANTEA (GI) partially fulfils these requirements; however, additional redundant factors are likely to contribute to Y's predicted functions (90, 91).

CCA1 and LHY belong to REVEILLE 1 to 8 (RVE1 to 8) subfamily of Myb transcription factors (125, 126). Recent characterizations of RVE1, CIRCADIAN 1 (CIR1/RVE2) and EARLY PHYTOCHROME RESPONSIVE 1 (EPR1/RVE7) revealed that their trends of expression are like CCA1 and LHY, peaking in subjective days close to dawn (125, 127, 128). This circadian expression depends on CCA1 and LHY and is likely mediated in their promoters by EE or EE - like motifs. Two FLAVIN BINDING KELCH F - BOX 1 (FKF1) and LOV KELCH PROTEIN 2 (LKP2) homologues also interact with TOC1 (66). ZTL, FKF1, and presumably LKP2, work as photoreceptors of blue light (66, 115). Light-related interaction between ZTL and GI stabilizes the protein levels of ZTL and TOC1 throughout the day. TOC1 is further stabilized by PSEUDORESPONSE REGULATOR 3 (PRR3), which binds directly to TOC1 in order to stop its early night direct interaction with ZTL (108, 121). Thus, a complex interaction between TOC1, ZTL, GI and PRR3 results in TOC1 degradation. Also, subject to proteasomal degradation are other clock components such as LHY (129) PRR7 (109), PRR9 (110) and GI (130). Whereas a RING-type E3-ubiquitin ligase tends to regulate the stability of GI during the night (64).

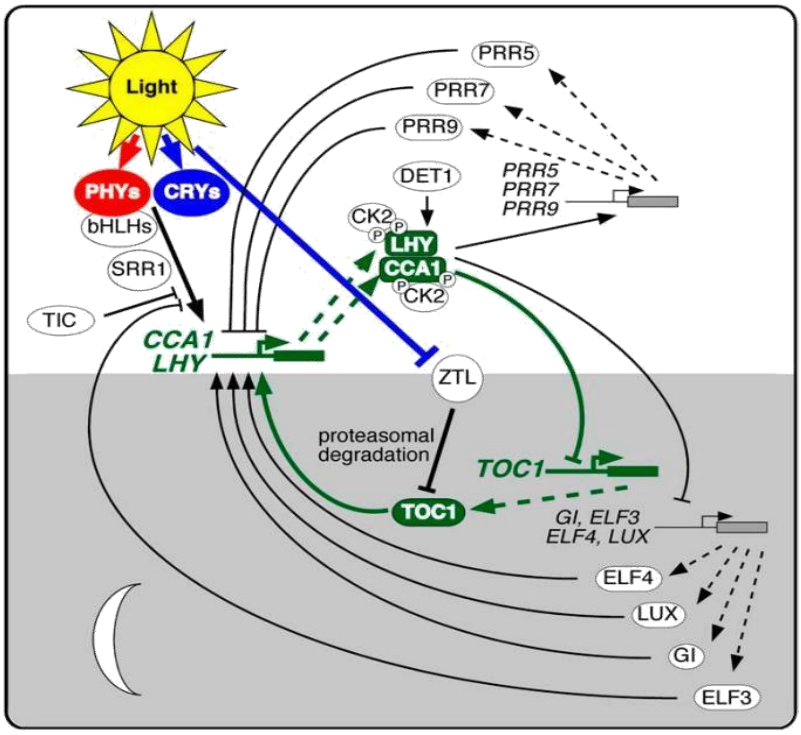

Figure 1-12. The molecular model of circadian clock in Arabidopsis. Genes are illustrated by solid boxes together with the gene names. Proteins with their names are illustrated by oval and oblong shapes. Protein activity is illustrated with solid lines. Lines ending in arrowheads indicating positive action and lines ending in perpendicular dashes indicating negative action. Dashed lines represent transcription and translation. The core CCA1/LHY/TOC1 feedback loop is highlighted by green thick lines. The grey area represents night-time, and the white area represent daytime (102).

1.9.2 Recent developments in Arabidopsis thaliana circadian clock

It is known that to activate the expression of PSEUDO-RESPONSE REGULATOR9 (PRR9) and PRR7, CCA1 and LHY are required (96), however, the molecular particulars of this stimulation remain secret. As part of a single feedback loop, CCA1 and LHY are specifically repressed by morning-expressed PRR9, midday-expressed PRR7, afternoon-expressed PRR5, and evening-expressed TOC1, thus forming a sustained set of repressive events extending from midday until around midnight (112, 131-133). Three other proteins associated with the clock, NIGHT LIGHTINDUCIBLE AND CLOCK-REGULATED GENE1 (LNK1), LNK2, and REVEILLE8 (RVE8), form complexes which activate afternoon PRR5 expression (134-137). PRR5 is induced in the afternoon by RVE8, but not in the morning, suggesting that repression exceeds the morning PRR5 transcription activation of LNK-RVE8. The exact repressive mechanism is not known (136). TOC1 and PRR5 were proposed as night-time PRR5 repressors based on earlier data (131, 138). More studies have indicated that the RVE8-LNK complex activates PRR5 transcription (135, 137) however, morning activation of RVE8- and LNK-

dependent PRR5 is highly reduced (136). This was found that CCA1 is associated with the PRR5 promoter in the morning, CCA1 and LHY suppress PRR5 transcription in the morning and PRR5 suppression in cca1 lhy double mutant plants is attenuated. Such observations suggest that CCA1 and LHY are potent morning PRR5 repressors as well as RVE8- and LNK- dependent transcriptional activation candidates (136).

Furthermore, nearly whole the discussion of clock regulation described to this point has been based on repression and hence Arabidopsis oscillator is modelled as repressilator (139). The observed suppression of PRR9 by the EC produces a three-negative feedback ring system in the framework of the whole clock circuit, called the repressilator (139). It has become apparent, nevertheless, more lately that several transcriptional activators are playing vital roles. LIGHT-REGULATED WD1 (LWD1) and LWD2 are multi-clock gene transcription co-activators, including CCA1, PRR9, PRR5, and TOC1(140-142). CCA1 promoter recruitment and transcription activation are mediated by the interaction between LWD1 and LWD2 with two CHE, TCP20 and TCP22-related TCP transcription factors (142). A role in CCA1 regulation is consistent with TCP20 transcript cycles with a pre-dawn maximum (143).

Three CCA1/LHY homologues, REVEILLE8 (RVE8), RVE4 and RVE6 include a second set of transcription activators subsequent than the TCP / LWD complexes (134, 136, 144). These RVEs create complexes with transcription coactivators, NIGHT LIGHT-INDUCIBLE AND CLOCK-REGULATED1 (LNK1), and LNK2 to activate PRR5, TOC1, and ELF4 expression (135, 137). Further ELF4 transcription activation is provided by FAR-RED ELONGATED HYPOCOTYL3 (FHY3), FAR-RED IMPAIRED RESPONSE1 (FAR1), and ELONGATED HYPOCOTYL5 (HY5), three positive phytochrome A transcription factors (145). The transcriptional repression activity of CCA1 and LHY is at least partially derived from their cooperation with and inactivation of FHY3, FAR1, and HY5 transcription modulation activity (145). It seems likely that added transcriptional regulators of central clock oscillator genes, both positive and negative, will remain to be detected and defined, further complicating a flourishing network of interconnected feedback loops (146).

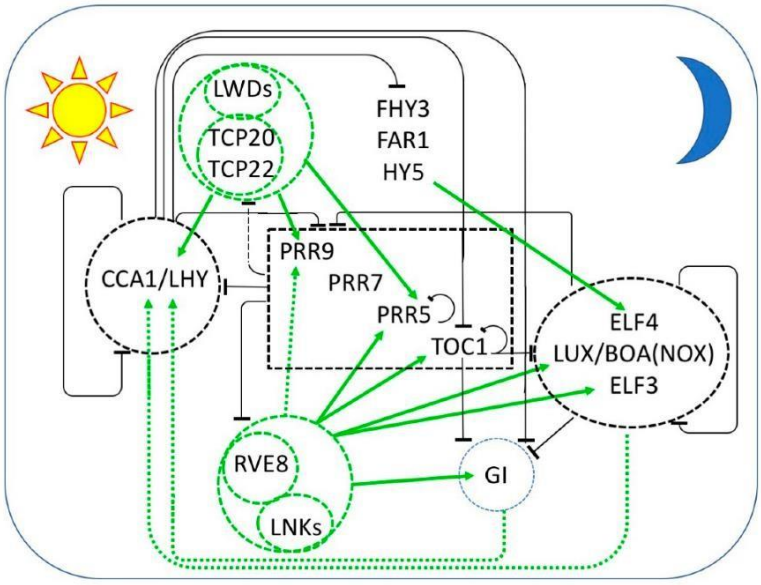

Figure 1-13. Multiple interlocked transcriptional feedback loops form the core of the circadian oscillator in Arabidopsis thaliana. The consecutive expression of each factor is shown from left to right all through the day / night cycle, with the morning portrayed by the sun on the left and the moon on the right. Black bars show repression and green arrows indicate transcription activation. Complexes of proteins are surrounded by dashed lines. Transcriptional activators are green and green arrows are used to indicate transcriptional activation. Dashed arrows show interactions that are not directly founded (146).

At dawn, the PRR genes, TOC1, GI, and EC members LUX, ELF3, and ELF4 are repressed by CCA1 and LHY. PRR9, PRR7, PRR5, and TOC1 are expressed sequentially, repressing the transcription of CCA1 and LHY and their transcription. LWD1 and LWD2 are co-activators recruited to DNA by TCP20 and TCP22 to promote CCA1, PRR9, PRR7 and TOC1 expression (146). The LNKs, DNA associated transcriptional coactivators by RVE8 (and probably RVE4 and RVE6) mediate transcriptional activation in the afternoon. RVE-LNK complexes promote PRR9, PRR5, TOC1 GI, LUX, and ELF4 transcriptions (146). FHY3, FAR1, and HY5 offer additional extra transcriptional activation of ELF4. TOC1 represses all the elements of the day as well as GI, LUX, and ELF4 in the evening (146). Together with ELF3, LUX and ELF4 form the evening complex (EC), a transcriptional GI, PRR9 and PRR7 repressor. The transcriptional activation of CCA1 and LHY appears to require GI and an EC variant containing BOA (NOX) (146).

2 Material and Methods

For simplicity's sake, computations were conducted using the LSODE subroutine of Fortran. Gnuplot plots have been generated (www.gnuplot.info). Concentrations of substances are represented by compound names without square brackets to make notes simpler. The ' dot ' notation demonstrates time derivatives. In arbitrary units (au), concentrations and parameter values are given. Rate parameters are presented as k_i's (i=1, 2, 3 ...) regardless of their dynamic character, i.e. whether they represent turnover numbers, constants of Michaelis, or constants of inhibition. The light induced on the model components is white light at a constant fluence rate. Several runs are performed for each individual model by adjusting the parameters, yet some of the graphs and data which have significant information and differences to be mentioned taken are shown.

3 Results and Discussion

3.1 Characterization of positive feedback

Alabadi et al. proposed a negative feedback loop between CCA1/LHY and TOC1, based on the mutual regulation that has been experimentally identified (46). CCA1/LHY and TOC1 are vital components, belonging to morning and evening loops respectively, forming the core loop.

Two molecular elements, A and E, are considered to influence the synthesis or degradation of each other by either activating them or inhibiting them (indicated by a dashed adverse inhibition symbol). The sort of feedback for a specific motif (i.e. positive or negative) can be determined as demonstrated in Figure 3-1(this example is motif 16 in Figure 3-3). Beginning with element A and proceeding along the loop while multiplying the plus / minus marks of the activation / inhibition phases with the positive / negative signs of the other component's synthesis/degradation response brings to the indication of the feedback loop that in the event of the motif in Fig 3-1 is positive. The controller motifs are built as follows: inhibition or activation stimuli from E and A act on the formation or degradation mechanisms of the other species, but not on both. Since A can impact E by four distinct methods (i.e. by activating or inhibiting the synthesis or degradation of E) and E can also affect A, we have 16 distinct motives in total. Eight of these are negative feedback loops in Figure 3-2, while the other eight are positive feedback Figure 3-3.

Based on the proposed relationship between morning and evening loops described by Nohales and Kay in 2016 (141), motif 16 (m16) was considered to observe how the model performs if changes are made in rate constants (147). For simplification, A represents morning loop while E is taken for evening loop in the figure. Model equations were established as mass balances using nonlinear ordinary differential equations in the form of kinetics from Michaelis – Menten and Hill.

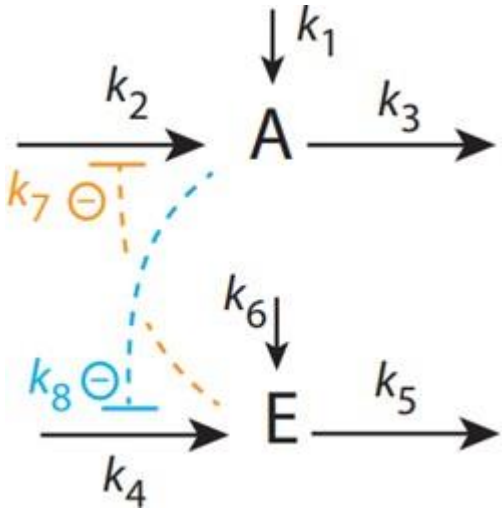

Figure 3-1. Positive feedback arrangement of motif 16.

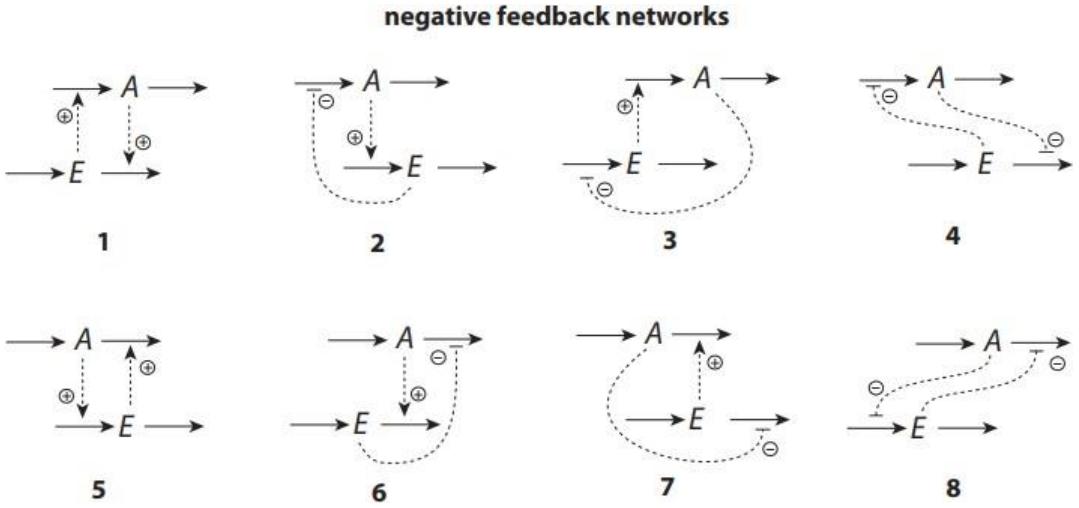

Figure 3-2. Network motifs with negative feedback (147).

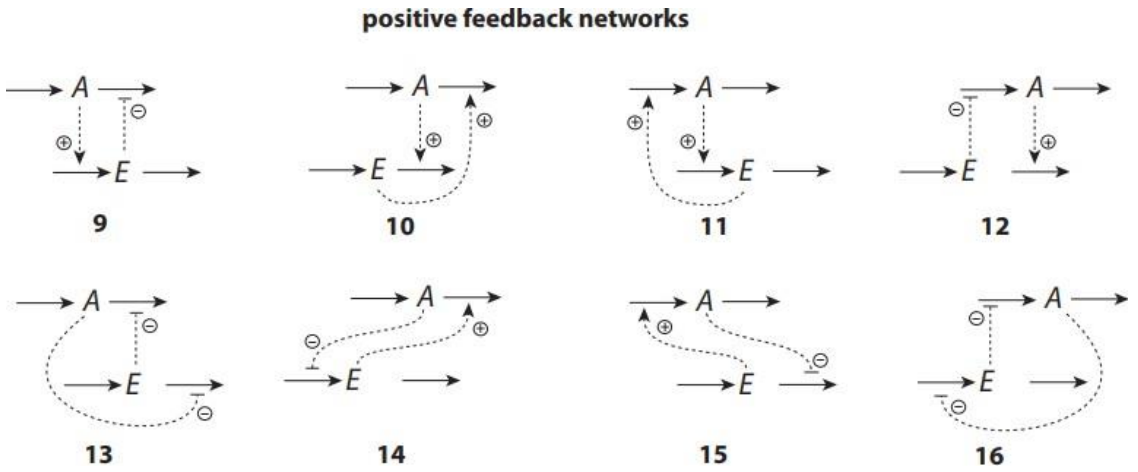

Figure 3-3. Network motifs with positive feedback (147).

The rate equations of this motif are

$$\dot{A} = k_1 + k_2 \left(\frac{k_7}{k_7+E}\right) - k_3.A \qquad (3.1)$$

$$\dot{E} = k_6 + k_4 \left(\frac{k_8}{k_8+A}\right) - k_5.E \qquad (3.2)$$

When using various combinations of constant rates, we will examine how m16 reacts as there can be different pattern of growth in A and E.

3.1.1 Logarithmic Growth of *E*

Initial run is performed in which k_3= k_5= k_6=0.0, while k_1= k_2=0.01, k_4=1.0, and k_7= k_8=0.1. Initial concentrations of *A* and *E* are zero.

With k_3=0, *A* increases with time, there is no steady state. Also, *E* increases and does not go into a steady state, but due to the inhibition by *A* and with k_6=0, the increase in *E*, which is only mediated by flux

$$j_4 = k_4 k_8 / (k_8 + A)$$

will slow down with increasing *A*. Since k_4 is 2-orders of magnitude larger than k_1 and k_2, *E* grows initially more rapidly than *A*, which means that the flux j_2= k_2 k_7 /(k_7+*E*) is much lower

than flux j_4. In fact, over the 400-time unit calculation A increases linearly, i.e., (see also Fig. 3.4)

$$\dot{A} = k_1 \Rightarrow A(t) = k_1 \cdot t + A\,(0) \tag{3.3}$$

```
1   HC71-01
2     0.0000E+00,  1.0000E-01,  400.0D+0,  0.0E+00,
3
4     1.00E-02        ** k1
5
6     1.00E-02       ** k2
7     0.00E+00        ** k3
8
9     1.00E+00        ** k4
10    0.00E+00        ** k5
11
12    0.00E+00        ** k6
13    1.0E-01         ** k7
14    1.0E-01         ** k8
```

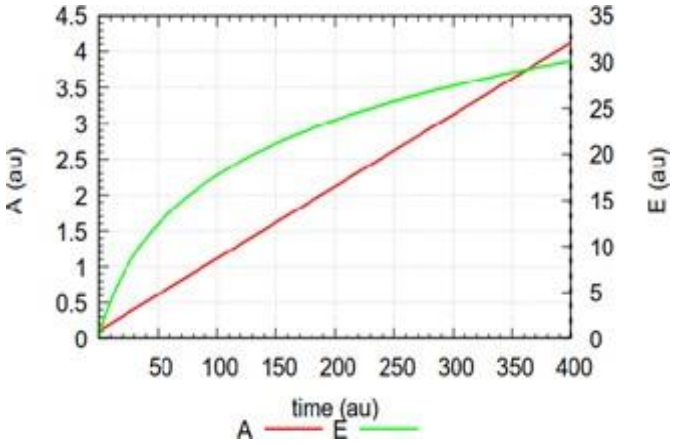

Figure 3-4. Output of HC7-01. Input parameters are given on left. i.e., the values for used for the rate constants. Note the linear and logarithmic curve fits of respectively A and E presented on the right.

With k_5=k_6=0.0 the rate equation of E becomes

$$\dot{E} \;=\; k_4 \left(\frac{k_8}{k_8 + A}\right) \tag{3.4}$$

Inserting $M(t) = k1 \cdot t$ from Eq. 3.3 (**note that** $A\,(0)$ **=0**), we get

$$\dot{E} = k_4 \left(\frac{k_8}{k_{8+1\cdot t}}\right) = k_4 \left(\frac{1}{1+\left(\frac{k_1}{k_8}\right)t}\right) \tag{3.5}$$

Integrating Eq. 3.5 give

$$E(t) = k_4 \int_0^t \left(\frac{d_t'}{1+\left(\frac{k_1}{k_8}\right)t'}\right) = k_4 \left(\frac{k_8}{k_1}\right) \int_{u=0}^{u=\left(\frac{k1}{k8}\right)t} \frac{du}{1+u} \tag{3.6}$$

where the following substitution has been made

$$u = \left(\frac{k_1}{k_8}\right) t' \rightarrow du = \left(\frac{k_1}{k_8}\right) dt' \rightarrow \quad dt' = \left(\frac{k_8}{k_1}\right) du \tag{3.7}$$

Integrating the right expression of Eq. 3.6 gives

$$E(t) = k_4\left(\frac{k_8}{k_1}\right) \int_0^{\left(\frac{k1}{k8}\right)t} \frac{du}{1+u} = k_4\left(\frac{k_8}{k_1}\right) \left[\log\left(1+\left(\frac{k_1}{k_8}\right)t\right) - \log(1+0)\right] + E(0) \quad (3.8)$$

which leads to the final expression for $E(t)$ (with E (0) = (0):

$$E(t) = \left(\frac{k_4 k_8}{k_1}\right) \cdot log\left(1+\left(\frac{k_1}{k_8}\right) \cdot t\right) \quad (3.9)$$

Inserting the rate constant values of run HC7-01 into Eq. 3.9 gives the expression

$$E(t) = 10.0 \cdot \log (1 + 0.1\ t) \quad (3.10)$$

which is in good agreement with the curve-fit of the numerical E - t data.

3.1.2 Doubling time τ of Logarithmic Growth

In order to calculate the doubling times τ we need to have nonzero initial concentrations A (0) and E (0).

This implies that $A.0/$ needs to be included in Eq. 1.4 leading to the alternative equation

$$\dot{E} = k_4\left(\frac{k_8}{k_8+k_1 \cdot t+A(0)}\right) = k_4\left(\frac{k_8}{k_8+A(0)+k_1 \cdot t}\right) = k_4 \cdot \frac{\left(\frac{k_8}{k_8+A(0)}\right)}{1+\frac{k_1}{k_8+A(0)} \cdot t} \quad (3.11)$$

Making the substitution $u = k_1/ (k_8 + A (0))$ with $dt = (k_8+A (0))/k_1 = dt$ and integration as in the previous section leads to

$$E(t) = \frac{k_4 k_8}{k_1} \cdot log\left(1+\left(\frac{k_1}{k_8+A(0)}\right) \cdot t\right) + E(0) \quad (3.12)$$

Using the same rate constant values as in HC7-01 with $A.0/=0:1$, Eq. 3.12 can be written as:

$$E(t) = 10.0 \cdot \log (1 + 0.05 \cdot t) + E\ (0) \quad (3.13)$$

The numerical coefficients in Eq. 1.13 are in good agreement with the curve-fit of the numerically calculated $E(t)$; see Figure. 3-5.

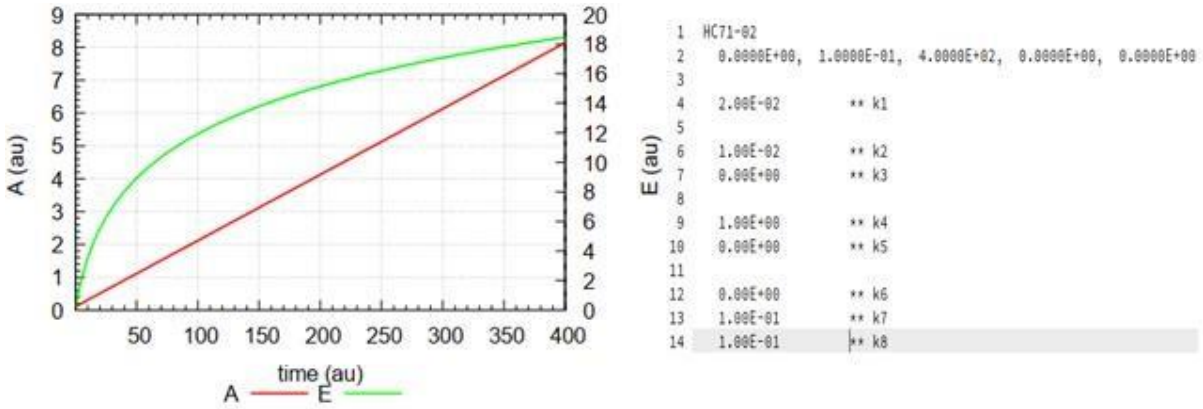

Figure 3-5. Output of run HC71-02.

3.1.3 Analytical Expression of the Doubling Time τ for Logarithmic Growth

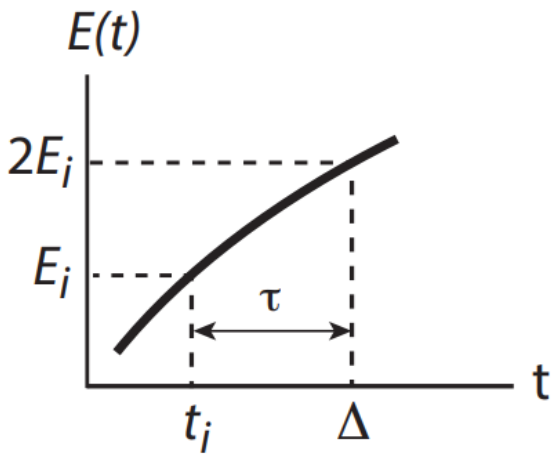

Figure 3-6. Defines the doubling time τ.

$E(t)$ increases with time. At time $t=t_i$ the con- centration of E is E_i. At time A the concentration of E has been doubled to $2E_i$. The time required to double E_i to $2E_i$ is the doubling time τ.

E follows the following equation with high precision

$$E(t) = \alpha \cdot \log(1 + \beta \cdot t) + E(0) \qquad (3.14)$$

At time t_i the concentration of E is

$$E(t_i) = \alpha \cdot log(1 + \beta \cdot t_i) + E(0) \qquad (3.15)$$

while at time Δ the concentration of E is $2E(t_i)$

$$2E(t_i) = \alpha \cdot log(1 + \beta \cdot \Delta) + E(0) \qquad (3.16)$$

Solving for t_i and Δ from equation 3.15 and 3.16 respectively, gives τ

$$t_i = \frac{1}{\beta}\left(e^{\frac{E(t_i)-E(0)}{\alpha}} - 1\right) \qquad (3.17)$$

$$\Delta = \frac{1}{\beta}\left(e^{\frac{2E(t_i)-E(0)}{\alpha}} - 1\right) \qquad (3.18)$$

Subtracting t_i from Δ gives τ, i.e.,

$$\tau = \Delta - t_i = \frac{1}{\beta}\left(e^{\frac{2E(t_i)-E(0)}{\alpha}} - 1\right) - \frac{1}{\beta}\left(e^{\frac{E(t_i)-E(0)}{\alpha}} - 1\right) \qquad (3.19)$$

Which can be written as

$$\tau = \frac{1}{\beta}e^{\frac{-E(0)}{\alpha}} \qquad (3.20)$$

Inserting into Eq. 3.19 the values for α =9.9176, β =0.049, and E (0) =0.1 (see Fig. 3.6), we get a very good agreement between the numerically calculated τ and the τ values calculated by Eq. 3.20

E(t) = α*ln(β*t+1) + E(0)

doubling time τ(E) (analytic) =[(e^(-E(0)/α))/β]*(e^(2*E /α)-e^(E /α))

E(t) = 9.9176*ln(1+0.049*t)+0.1 ; see run HC7-02
fac=(1/0.0490)*exp(-0.1/9.9176)

E	tau analytic	tau num calc
1.00E-01	2.07E-01	2.01E-01
2.00E-01	4.20E-01	4.11E-01
4.00E-01	8.66E-01	8.52E-01
8.00E-01	1.84E+00	1.82E+00
1.60E+00	4.16E+00	4.13E+00
3.20E+00	1.06E+01	1.06E+01
6.40E+00	3.49E+01	3.50E+01
1.28E+01	1.94E+02	1.94E+02

Figure 3-7. Comparing the numerically and analytically calculated τ's

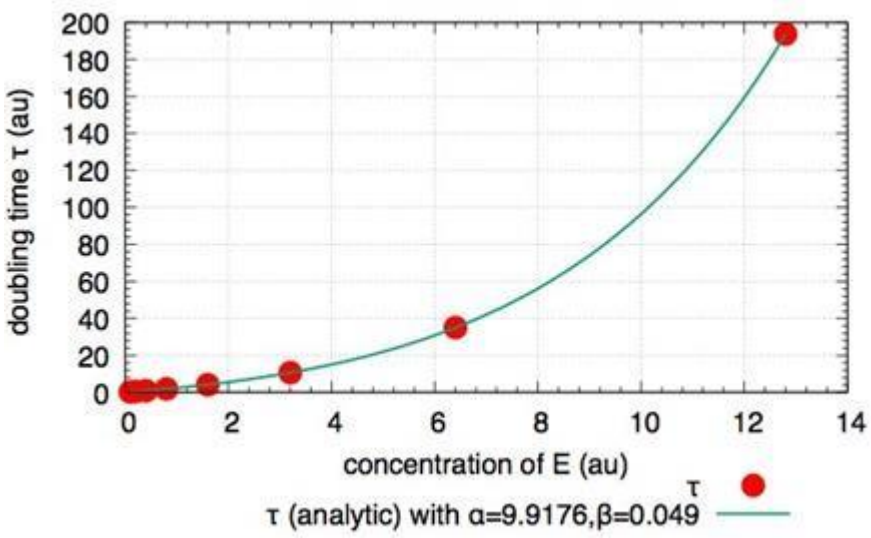

Figure 3-8. Plot of the numerically and analytically calculated τ's.

Change of rate constant *k*1

As HC7-02, but $k_1 = 0$. Only *A* and *E* are shown without precise calculation of the τ and its functional description. No *A* is made through k_1 and no *E* is made through k_6. *E* is increasing linearly, while *A* has an apparent logarithmic increase. The larger rate (and linear) increase in *E* appears due to the larger value of k_4 (1.0) in comparison with the lower value of k_2 (0.01).

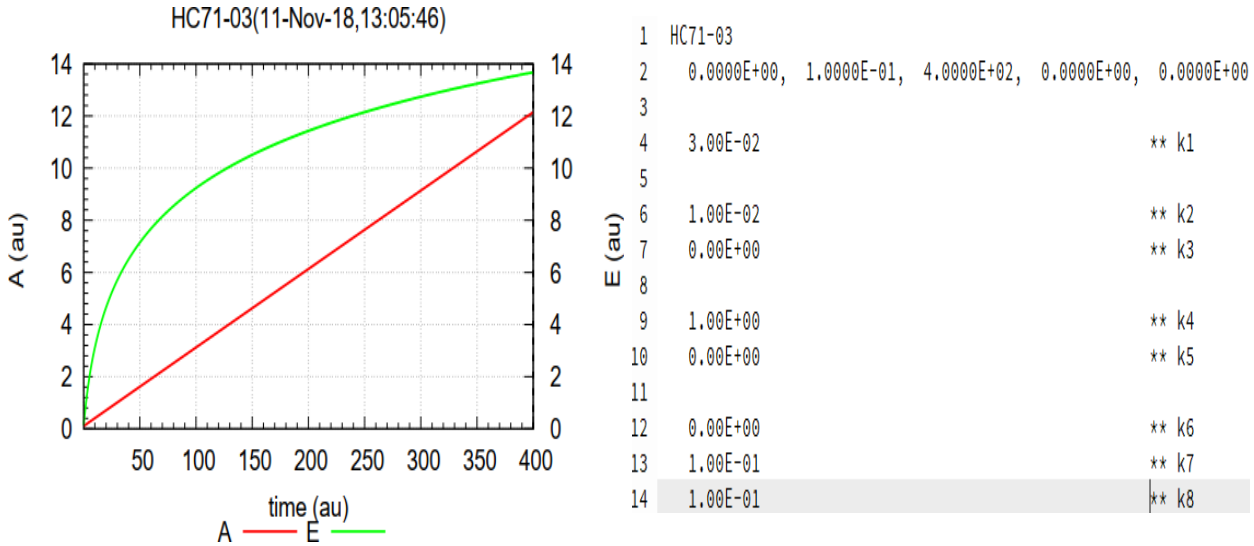

Figure 3-9. Results of run showing the increase of A and E.

The doubling time of *A* cannot be calculated here as the initial value of 0.1 for *A* is too large and the logarithmic growth of *A* would take a very long time to reach 0.2.

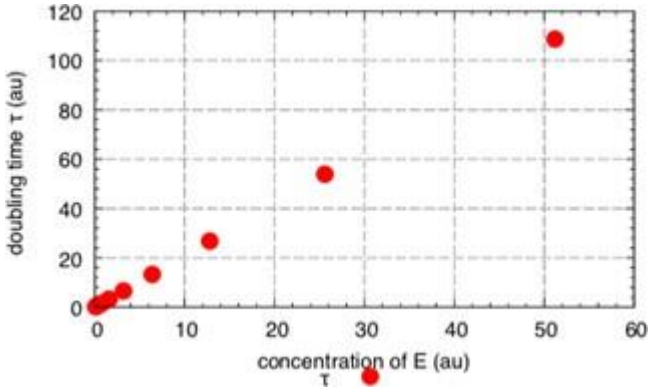

Figure 3-10. Results of HC7-03 showing the linearly doubling of E.

3.2 Compact Models for *Arabidopsis thaliana*

Mathematical modelling has been used over the past decade to comprehend the clock's intricate details in the *Arabidopsis thaliana* model plant. These efforts have produced a series of increasingly sophisticated models. Several models were taken into consideration to be used in the calculations as previous models presented varying results. Despite their independent evolutionary origins, eukaryotic clocks rely on transcription and translation-based feedback loops in cases where the molecular basis is known (82). While the complexity of the individual elements of the clockwork may differ, the overall structure of the network is maintained across kingdoms (102).

The proper sensing and integration of these environmental signals are particularly relevant for plants, as their sessile nature necessarily limits their ability to avoid challenging conditions. In this work, we discuss existing knowledge of how the environment sets the pace of the clock and incorporate recent progress in understanding the molecular mechanisms that shape the oscillator in the Arabidopsis thaliana model plant (141). Here an alternative model is presented by combining a small number of equations and parameters, like the very earliest models, with the complex network structure found in newer ones.

3.2.1 3LM: Three loop model

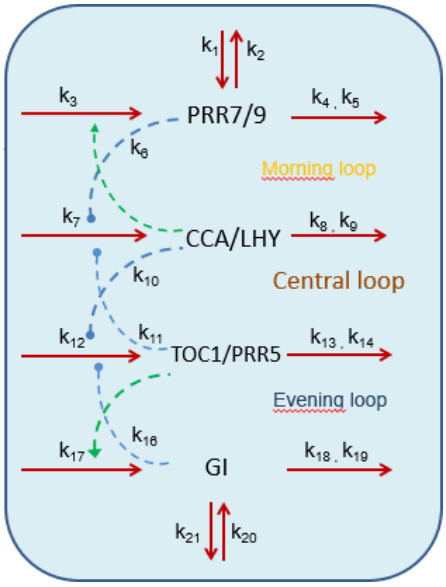

Figure 3-11. Schematic representation of Model 3LM based on the previous models discussed in previous research papers.

The model has been given the name of 3LM (three loop model). Although name three loop model is used, yet not all models are strictly three loop models. This model has been built by first letting the morning and evening loop oscillate in isolation by finding similar parameters as in the ML program but using only two intermediates (calculations not shown). The evening loop is made then by using the same rate parameters as for the morning loop and checking that the two oscillators behave consistently. CCA and LHY are grouped together as CCA/LHY while TOC1 and PRR5 are taken as single component (141) in evening loop. Finally, the morning and evening loops are coupled together by the feedback motif m16, which forms the inner loop.

The following rate equations are derived for the model to explain morning and evening loops and different parameters affecting the clock.

$$\frac{dPRR7/9}{dt} = k_1 - k_2 \cdot PRR7/9 - \frac{k_4 PRR7/9}{k_5 + PRR7/9} + k_3 \cdot CCA/LHY$$

$$\frac{dCCA/LHY}{dt} = k_7 \left[\left(\frac{k_6}{k_6 + PRR7/9}\right) \cdot \left(\frac{k_{11}}{k_{11} + TOC1/PRR5}\right)\right] - \frac{k_8 \cdot CCA/LHY}{k_9 + CCA/LHY}$$

$$\frac{dTOC1/PRR5}{dt} = k_{12} \left[\left(\frac{k_{10}}{k_{10} + CCA/LHY}\right) \cdot \left(\frac{k_{16}}{k_{16} + GI}\right)\right] - \frac{k_{13} \cdot TOC1/PRR5}{k_{14} + TOC1/PRR5}$$

$$\frac{dGI}{dt} = k_{17} \cdot \frac{TOC1}{PRR5} - \frac{k_{18} GI}{k_{18} + GI} + k_{20} - k_{21} \cdot GI$$

The calculations are done for this model by running the program for several time and given the name of 3LM-01, 3LM-02 and further subsequently in this manner. If the inhibition constants between CCA/LHY and TOC1 are chosen not too strong, then oscillations without beating can be observed as in Figure 3-12. The period is measured by PRR7/9 variable. The period of three loop model appears longer than the period of the single morning and evening loop oscillators.

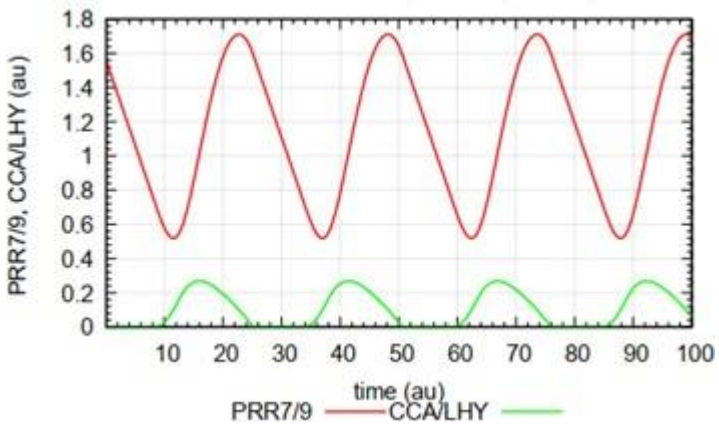

Figure 3-12. Shows oscillatory behaviors of peaks without beating and with comparatively large period.

Another run was performed by using the same initial concentration and rate parameter values as in previous calculation 3LM-01. This can be seen in figure 6-3 that the oscillations for the pairs PRR7/9 and GI and oscillations for TOC1 and CCA/LHY have the same amplitude yet approximately 180 out of phase to each other.

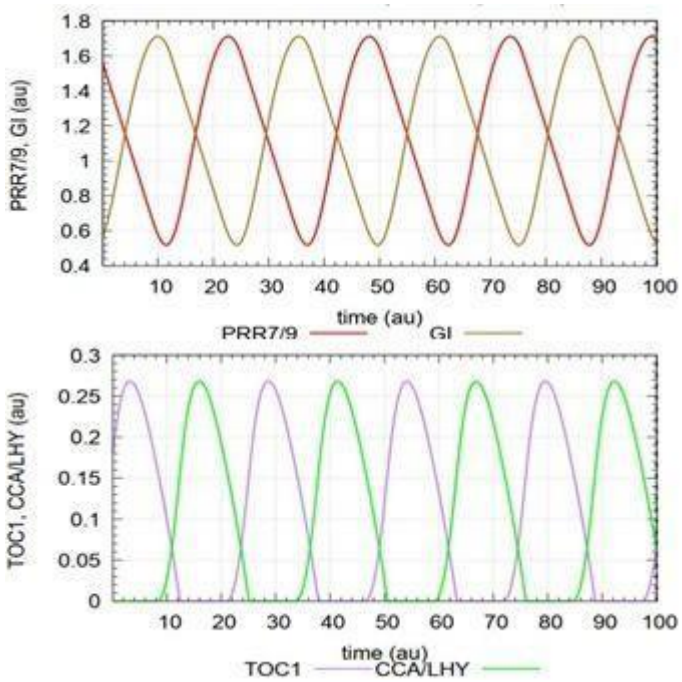

Figure 3-13. Represents opposite phasing for both morning and evening loop oscillator components.

Another observation was made that increasing the rate parameter k4 results in an increase in amplitude PRR7/9 in comparison to both GI and rose in CCA/LHY compared to TOC1. While not any significant effect not seen on the period like isolated PRR7/9-CCA/LHY negative feedback loop.

The program is used to make another run in which k_{18} in the GI-TOC1 loop is increased from 0.1 to 0.2. Analogues behaviors are repeated as was observed for the previous run. TOC1/GI has increased amplitude while PRR7/9-CCA/LHY amplitude appears to be unaffected. The period is slightly affected that can be seen in 3LM-04.

Once more, modification is made in the degradation parameter of the model k_8, which is increased from 0.09 to 0.18. In this case, one can observe splitting in PRR7/9-CCA/LHY oscillations showing two periods. TOC1/GI has single oscillations while the period, in this case, is decreased.

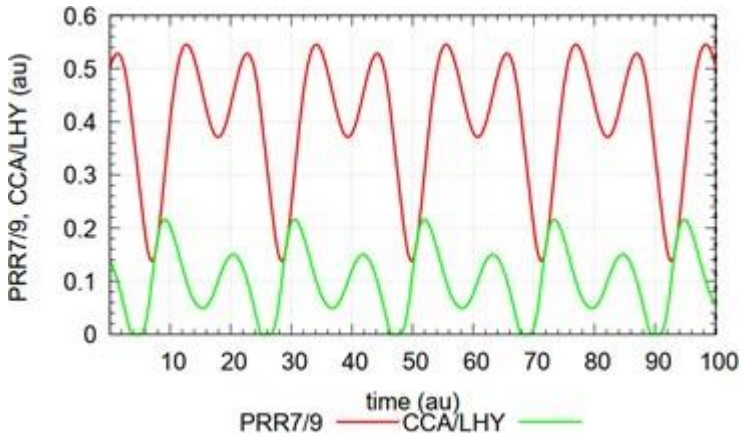

Figure 3-14. Splitting pattern showing double peaks with relatively short period length.

The next run is performed by returning the value of k_8 to 0.09 while k_{13} is raised to 0.18, double of the previous run. These changes once again result in analogous behavior than the previous run. The oscillations for the loop PRR7/9-CCA/LHY are unaffected while the TOC1/GI show "splitting." The period is also decreased in this case.

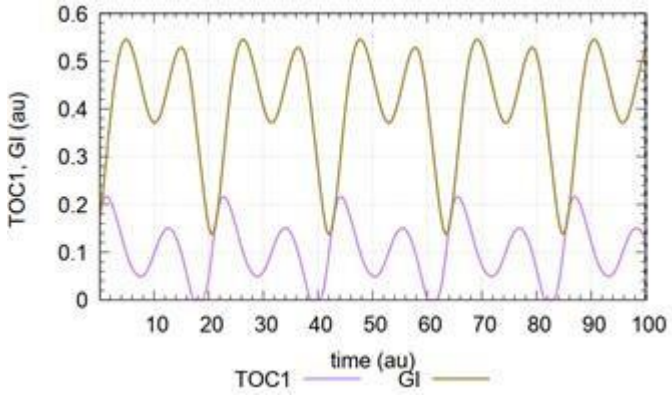

Figure 3-15. TOC1 and GI showing splitting with decreased period length.

Further by using the same parameters as used for 3LM-02 while k_3 is increased from 0.1 to 0.2. There is not any change in the form of oscillations, i.e. splitting, but the period length is decreased. To explain this for k_3=1, the period length was ahead 25 hours while if k_3 =2 the period is reduced to about 20 hours.

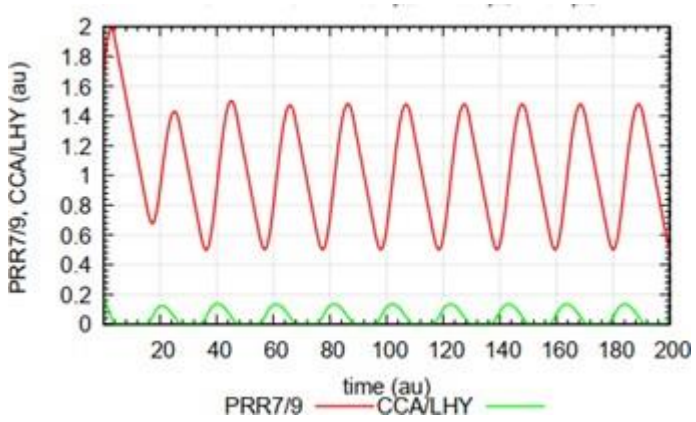

Figure 3-16. Reduced period length to 20 hours if k_3 =2, not changing the other parameters.

The next step is performed by taking the initial value for k_3, while rate constant k_7 is set to 2. A slight increase in the period. Is observed rising to 28 hours from 25 hours, which was noted when a value for k_7 was kept to 1. The oscillation shows a pattern with alternative high and low peaks both in PRR7/9 and CCA/LHY.

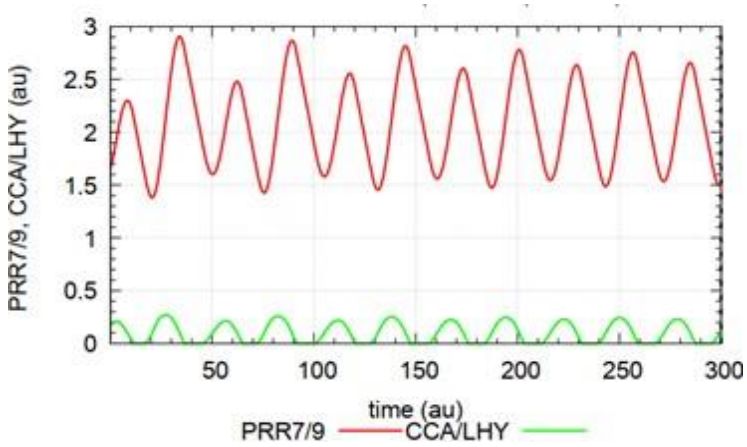

Figure 3-17. Oscillation showing a distinct alternative repeating peak with relatively larger period length.

A simple modification is done in the previous run to see the effect of the increased period; hence,

the oscillations were recorded after 1000-time units. It was seen that the alternative peaks disappeared, and oscillations become standard with the same period of about 28 hours. (not shown).

3.2.2 Model 3LM2

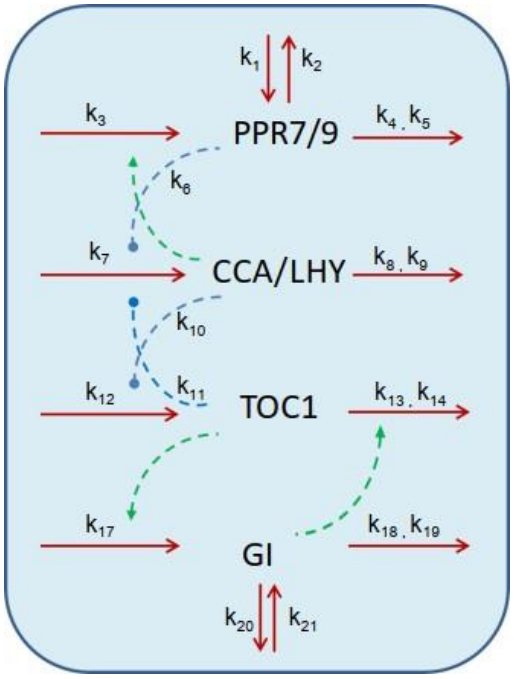

Figure 3-18. Model 3LM2 representing mutual activation between TOC1/PRR5 and GI

The structure of 3LM2 (second, three loop model) is given above. This model assumes that GI contributes to the degradation of TOC1/PRR5 through ZTL (148, 149), in contradiction to model 3LM where GI enhanced TOC1/PRR5. It was observed that the phasing is not much changed if compared to the previous model.

The rate equations are written in LSODE/Fortran code.

$$\frac{dPRR7/9}{dt} = k_1 - k_2 \cdot PRR7/9 \ + k_3 \cdot CCA/LHY - \frac{k_4 PRR7/9}{k_5 + PRR7/9}$$

$$\frac{dCCA/LHY}{dt} = k_7 \left[\left(\frac{k_6}{k_6 + PRR7/9}\right) \cdot \left(\frac{k_{11}}{k_{11} + TOC1}\right)\right] - \frac{k_8 \cdot CCA/LHY}{k_9 + CCA/LHY}$$

$$\frac{dTOC1/PRR5}{dt} = k_{12} \left[\left(\frac{k_{10}}{k_{10} + CCA/LHY}\right)\right] - GI \ \cdot \frac{k_{13} \cdot TOC1/PRR5}{k_{14} + TOC1/PRR5}$$

$$\frac{dGI}{dt} = k_{17} \cdot \frac{TOC1}{PRR5} + k_{20} - k_{21} \cdot GI \ - \frac{k_{18} GI}{k_{18} + GI}$$

To get the oscillations the rate constants of the TOC1/GI had to be changed slightly. Like PRR7/9-CCA/LHY oscillator, the TOC1-GI oscillator is a conservative system and show harmonic oscillations. The following runs are performed for model 3LM2 and given name 3LM2-01 and likewise.

The following rate constants are used to perform the first run 3LM2-01 for this model.

$$k_1 = k_2 = k_{20} = k_{21} = 0$$

$$k_3 = k_7 = k_{12} = k_{17} = 1$$

while the output constants are given these values k_4=0.1, k_8=0.09, k_{13}=0.1, k_{18}=1

$$k_5 = k_9 = k_{14} = k_{19} = 10^{-6}.$$

The inhibition constants were given these values for this run.

$$k_6 = 0.1,\ k_{10} = 1.0,\ k_{11} = 5$$

In next run 3LM2-02 morning and evening loops were uncoupled, i.e., the values of k_{10} and k_{11} are high both 1×10^{6}. The period determination of the morning and evening loop oscillations is also implemented in this run. In addition, the theoretical estimates of the period lengths of isolated loops were also provided.

The evening loop oscillator can be described by the following equation.

$$\text{TOC1} = A sin(\omega . t + \varphi) + \text{TOC1}_{set}$$

While the period length is approximated by harmonic average.

3.2.2.1 Analytical expression for the oscillations of evening loop

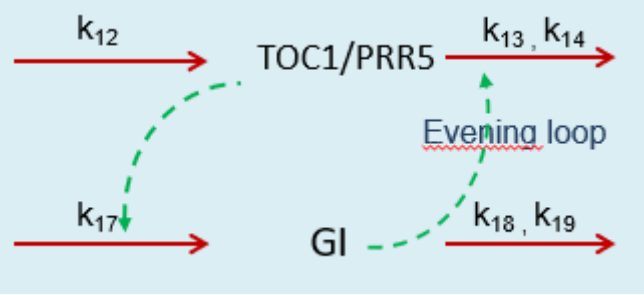

Figure 3-19. Evening loop in which TOC1/PRR5 has positive activation on GI.

$$(\dot{TOC1/PRR5}) = k_{12} - (GI) \cdot \frac{k_{13} \cdot TOC1/PRR5}{k_{14} + TOC1/PRR5}$$

Since $k_{14} \ll TOC1/PRR5$, so

$$\frac{TOC1/PRR5}{k_{14} + TOC1/PRR5} = 1$$

And

$$\dot{TOC1}/PRR5 = k_{12} - GI \cdot k_{13}$$

$$\dot{GI} = k_{17} \cdot TOC1/PRR5 - K_{18} \frac{GI}{k_{19} + GI}$$

While $\frac{GI}{k_{19}+GI} = 1$

Taking the double derivative of TOC1

$$(\ddot{TOC1}/PRR5) = \dot{GI} \cdot k_{13}$$

$$(\ddot{TOC1}/PRR5) = -(k_{17} \cdot TOC1/PRR5 - k_{18}) \cdot k_{13}$$

Rearranging the equation and further calculation results in the following equation.

$$\frac{\ddot{TOC1}/PRR5}{k_{13}k_{17}} + \ TOC1/PRR5 \ = \frac{k_{18}}{k_{17}} = TOC1/PRR5_{set}$$

The above equation is that of harmonic oscillation.

While given the steady state concentration for $TOC1/PRR5$

$$(TOC1/PRR5_{ss}) \ = TOC1/PRR5_{set} \ = \frac{k_{18}}{k_{17}}$$

The above equations are in accordance with the harmonic oscillation equation. i.e.

$$\frac{\ddot{x}}{\omega^2} + x = x_0$$

The variation in TOC1 with time is given as

$$A\,sin(\omega \cdot t + \varphi) + TOC1/PRR5_{set}$$

$$P = \frac{2\Pi}{\omega}$$

This gives

$$\dot{TOC1/PRR5} = A \cdot \omega\, cos(\omega \cdot t + \varphi)$$

$$\frac{d^2}{dt^2} = \ddot{TOC1/PRR5} = -A \cdot \omega^2\, sin(\omega \cdot t + \varphi)$$

$$\frac{\ddot{TOC1/PRR5}}{\omega^2} = -A\,sin(\omega \cdot t + \varphi) = TOC1/PRR5_{set} - TOC1/PRR5(t)$$

$$\frac{\ddot{TOC1/PRR5}}{\omega^2} + TOC1/PRR5 = TOC1/PRR5_{set}$$

$$\omega = \sqrt{k_{13}.k_{17}}$$

$$P = \frac{2\Pi}{\sqrt{k_{13} \cdot k_{17}}}$$

This expression for the period of the isolated TOC1-GI oscillator is incorporated into the program 3LM2.

3.2.2.1 Analytical estimate of the period of the morning loop

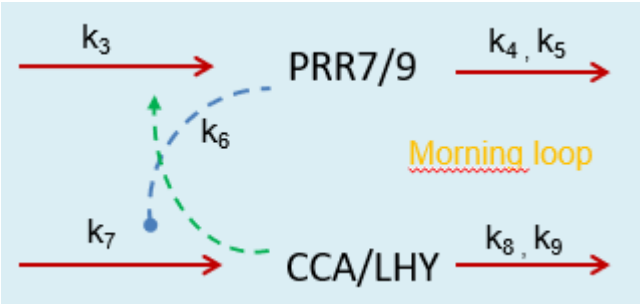

Figure 3-20. Morning loop have inverse relation between PRR7/9 and CCA/LHY

$$\dot{PRR7/9} = k_3(CCA/LHY) -\cdot \frac{k_4 \cdot PRR7/9}{k_5 + PRR7/9}$$

$$\dot{CCA/LHY} = k_7(\frac{k_6}{k_6 + PRR7/9}) - K_8 \frac{CCA/LHY}{k_9 + CCA/LHY}$$

Taking the double time derivative of CCA/LHY

$$CCA/LHY = \frac{-k_7 k_6}{(k_6 + PRR7/9)^2} \cdot \dot{PRR7/9}$$

$$= -\frac{k_6 k_7}{(k_6 + PRR7/9)^2}[k_3 \cdot CCA/LHY - k_4]$$

Rewriting the equation as

$$\ddot{CCA/LHY} + \frac{k_3 k_6 k_7}{(k_6 + PRR7/9)^2}\ CCA/LHY = \frac{k_4 k_6 k_7}{(k_6 + PRR7/9)^2}$$

Multiplying the above equation with $\frac{1}{\frac{k_3 k_6 k_7}{(k_6+PRR7/9)^2}}$ results in

$$\frac{\ddot{CCA/LHY}}{\frac{k_3 k_6 k_7}{(k_6+PRR7/9)^2}} + CCA/LHY = \frac{k_4}{k_3} = CCA/LHY_{\text{set}}$$

CCA/LHY_{set} is derived from the $\dot{PRR7/9} = 0$

$$k_3(CCA/LHY) - k_4 = 0$$

$$CCA/LHY_{\text{set}} = \frac{k_4}{k_3}$$

Frequency then was identified by the following relationship.

$$\omega^2 = \frac{k_3 k_6 k_7}{(k_6 + PRR7/9)^2}$$

Inserting the steady state or average value for $(PRR7/9)$, the estimate of frequncy for morning oscillators.

The steady state value of PRR7/9 can be calculated from the $\dot{CCA/LHY}$. Equation

$$\frac{d}{dt} = \dot{CCA/LHY} = \frac{k_6 k_7}{(k_6 + p)} - k_8 = 0$$

$$k_6 k_7 = k_8(k_6 + PRR7/9_{ss})$$

$$(PRR7/9_{ss}) = k_6\left(\frac{k_7}{k_8} - 1\right)$$

Inserting $(PRR7/9_{ss})$ into $\omega^2 = \frac{k_3 k_6 k_7}{(k_6+PRR7/9)^2}$ leads to the frequency

$$\omega = \sqrt{\frac{k_3 k_6 k_7}{(k_6 + PRR7/9)^2}}$$

$$P = \frac{2\pi}{\omega}$$

This equation is also implemented in the program 3LM2.

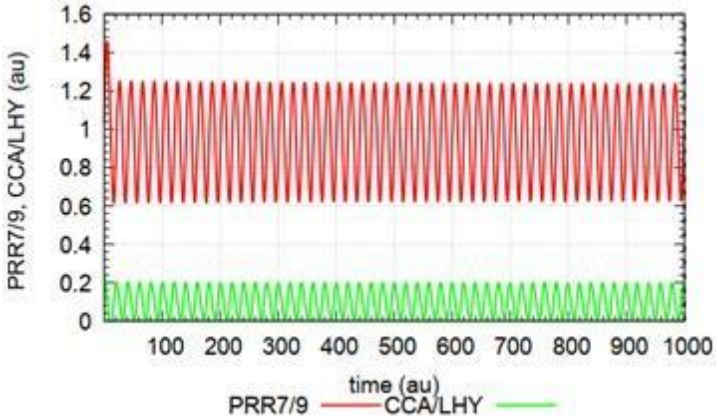

Figure 3-21. The output of the run 3LM2-02 is shown. Morning and evening loops are uncoupled with relatively high values for k_{10} and k_{11}.

The run is performed by using the rate constants as given below so both loops are decoupled.

$$k_1 = k_2 = k_{20} = k_{21} = 0$$
$$k_3 = k_7 = k_{12} = k_{17} = 1$$

while

$$k_{10} = k_{11} = 1x10^6$$

The period length obtained for both decoupled oscillators agrees with the numerical values.

3LM2-03 is performed by increasing the value of k_{13} from 0.01 to 0.1. Both decoupled oscillators have a period of about 19.87 hours. While in the next run 3LM2-04 entrainment of both oscillators can be observed by one another if the value of k_{10}=0.5 and k_{11}=2.0.

In run 3LM2-06 k_{10} is decreased from 0.5 to 0.2, i.e., the inhibition of TOC1-GI oscillator by the PRR7/9 has become stronger. This caused a further increase in period length to 24.1 hours.

The oscillations at t=0 start at the peak level of CCA/LHY. A slight increase in amplitude was measured for TOC1/PRR5, PRR7/9 and GI, which can be seen in the figure.

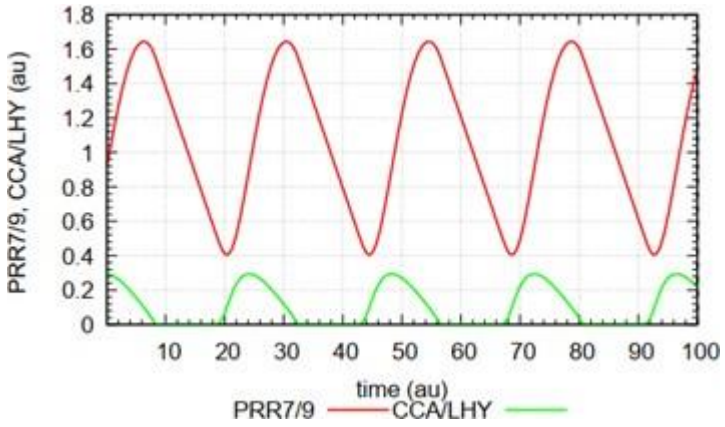

Figure 3-22. The inhibition of evening oscillator becomes stronger by PRR7/9-CCA/LHY with an increased period length. Peak for CCA/LHY appears earlier than PRR7/9 as described by Nohales and Kay (103).

3.3 Model 3LM3

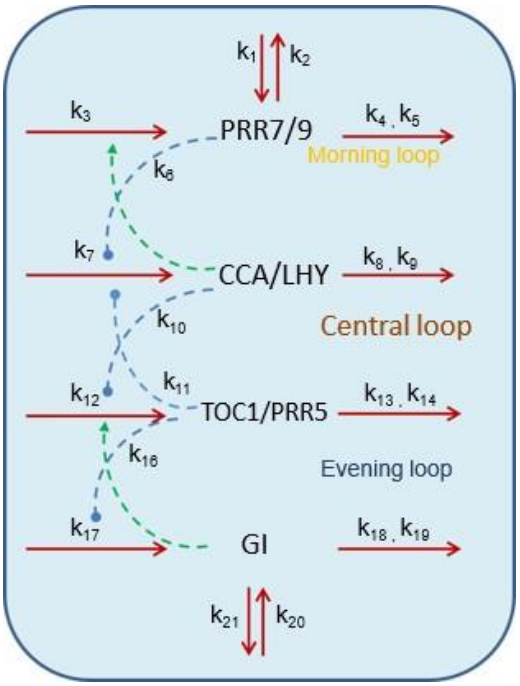

Figure 3-23. Model 3LM3.

Contrary to 3LM1 and 3LM2, it assumed this time that GI acts as activator of TOC1/PRR5 while morning and evening oscillators are combined with positive feedback relationship. The morning loop arrangement is taken as such also in this model.

$$PRR7/9 = k_1 - k_2 \cdot PRR7/9 \ + k_3 \cdot CCA/LHY - \frac{k_4 PRR7/9}{k_5 + PRR7/9}$$

$$\mathrm{CCA/LHY} = k_7 \left[\left(\frac{k_6}{k_6 + PRR7/9}\right) \cdot \left(\frac{k_{11}}{k_{11} + TOC1/PRR5}\right)\right] - \frac{k_8 \cdot CCA/LHY}{k_9 + CCA/LHY}$$

$$TOC1/PRR5 = k_{12} \left[\left(\frac{k_{10}}{k_{10} + CCA/LHY}\right)\right] GI \ - \frac{k_{13} \cdot TOC1/PRR5}{k_{14} + TOC1/PRR5}$$

$$GI = k_{17} \cdot \left(\frac{k_{10}}{k_{10} + CCA/LHY}\right) + k_{20} - k_{21} \cdot GI \ - \ k_{18} \cdot GI$$

3.3.1 Estimating the period of the TOC1/GI oscillator in Isolation

$$\frac{d}{dt} = \dot{TOC1/PRR5} = k_{12} - (GI) \cdot \frac{k_{13} \cdot TOC1/PRR5}{k_{14} + TOC1/PRR5}$$

$$\frac{d}{dt} = \dot{GI} = k_{17} \cdot (\frac{k_{16}}{k_{16} + TOC1/PRR5}) - K_{18} \frac{GI}{k_{19} + GI}$$

$$\frac{d^2}{dt^2} = \ddot{GI} = -\frac{k_{17}k_{16}}{k_{16} + TOC1/PRR5} \cdot TOC1/PRR5$$

$$\ddot{GI} + \frac{k_{17}k_{16}}{k_{16} + TOC1/PRR5} (k_{21} \cdot GI - k_{13}) = 0$$

$$\ddot{GI} + \frac{k_{17}k_{16}}{k_{16} + TOC1/PRR5} \cdot GI = \frac{k_{13}k_{16}k_{17}}{(k_{16} + TOC1/PRR5)^2}$$

Dividing by $\frac{k_{12}k_{16}k_{17}}{(k_{16}+TOC1/PRR5)^2}$ gives

$$\frac{\frac{\ddot{GI}}{k_{12}k_{16}k_{17}}}{(k_{16} + TOC1/PRR5)^2} + GI = \frac{k_{13}}{k_{12}} = GI_{set}$$

$$\frac{k_{12}k_{16}k_{17}}{(k_{16} + TOC1/PRR5)^2} = \omega^2$$

With $P = \frac{2\pi}{\omega}$ Calculating the average TOC1 lead to TOC1ss by setting GI=0

$$\frac{k_{16}k_{17}}{(k_{16} + TOC1/PRR5)} = k_{18}$$

$$(\frac{1}{k_{16} + TOC1/PRR5})^2 = (\frac{k_{18}}{k_{16}k_{17}})^2$$

$$\frac{k_{12}k_{16}k_{17}\ k_{18}^2}{k_{16}^2 k_{17}^2} = \frac{k_{12}k_{16}k_{17}}{(k_{16} + TOC1/PRR5)^2} = \omega^2$$

$$\omega = \sqrt[k_{18}]{\frac{k_{12}}{k_{16} \cdot k_{17}}}$$

$$P = \frac{2\pi}{k_{18}\sqrt{\frac{k_{12}}{k_{16} \cdot k_{17}}}}$$

Calculation of the both PRR7/9-CCA/LHY and TOC1/PRR5-GI oscillators is done by taking k_{10}= k_{11}=0.1 which gives strong coupling between oscillators. The period is significantly higher in this run than the period of individual oscillators. Using the same parameters for the run, 3LM3-03 was done starting with CCA/LHY peak at t=0. The GI peak now came before the TOC1 peak.

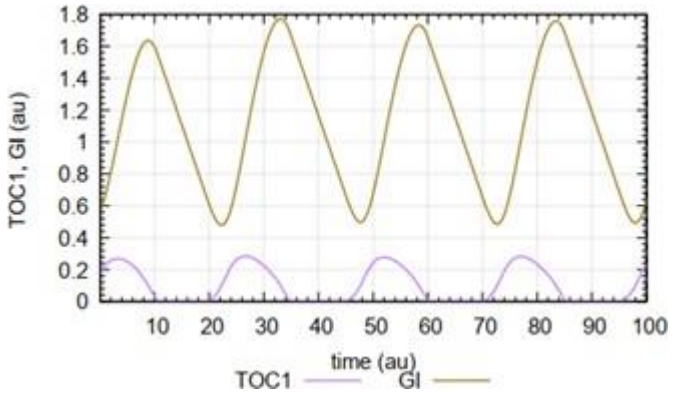

Figure 3-24. The run 3LM3-03 showing that GI peak comes before TOC1 peak.

When the value for the same rate constants is increased to 0.2, in 3LM3-04, morning loop oscillations become complex while evening loop shows simple oscillations which also appear to be regular, i.e. the oscillatory pattern repeats. If the values of mutual inhibitory rate constants k_{10}=0.5 and k_{11}=2.0, the oscillations in GI are regular with the period of about 21.9 hours while PRR7/9 oscillator has a shorter period of just 8.5 hours as can be seen in 3LM3-05.

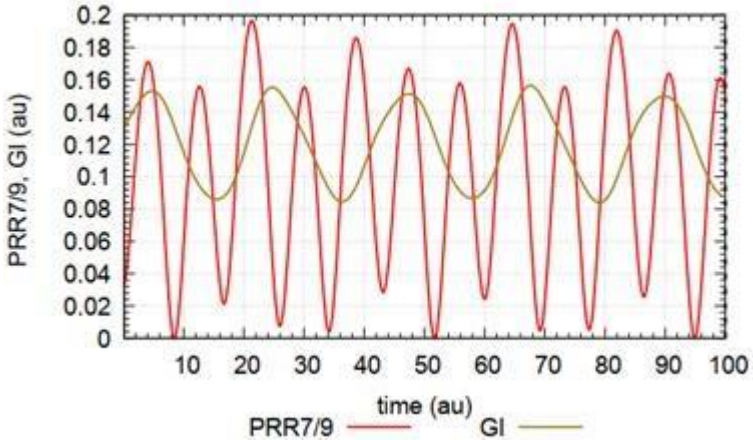

Figure 3-25. The GI oscillations are regular with period of about 22 hours in comparison to PRR7/9 oscillations with very short period.

3LM3-06 was performed by taking k_{10}=1 while k_{11}=0.2. The inhibition of evening oscillator by morning loop is weaker than the inhibition evening loop has on morning oscillator. The morning oscillator has a much short period, and the oscillations are complex. The same parameters are used in the next run while going up to 400 times units. Although the evening oscillations look simpler, they have a similar pattern which regularly repeats about every 100-time units.

3LM3-08 has different values for k_{10} and k_{11}, which were used for 3LM3-06. The GI oscillations are still regular while PRR7/9 oscillations show splitting. Morning oscillator has a period of about 19.9 hours while that of evening oscillator is nearly 30.2 hours. Similarly, in the next run, the value of k10 is increased to 0.5. With this change, the oscillations in PRR7/9 becomes less, although there are different peak types in the oscillations.

The next couple of tests were done by keeping the values of k_{10}= k_{11}=0.1, and the oscillations become regular characterized by simple circuit cycle. Using the same conditions as in 3LM3 ten while the initial values of TOC1/GI oscillator are those at time t=10. The response becomes quite chaotic concerning the maximum point of GI. Figure 6-16 shows the first 200-time units.

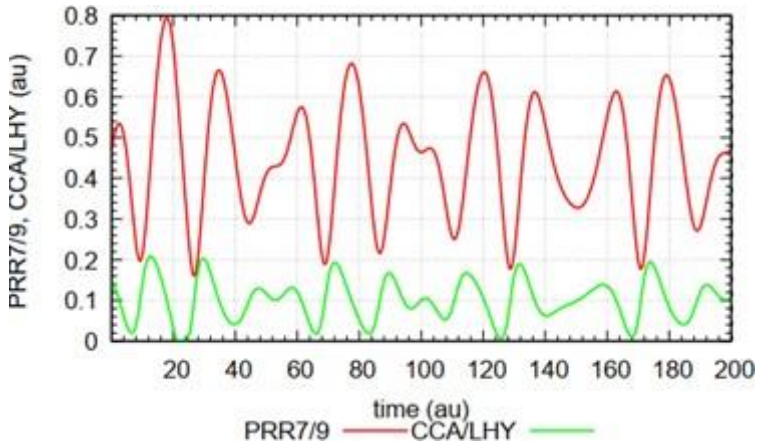

Figure 3-26. A chaotic response is shown in this run of model 3LM3.

Then decided to get output till 1000-time units in next run. Complex oscillations still can be seen quite some time yet. The time units are further increased to 10000. In the run 3LM3-13, oscillations have now regained the same relative phasing as the calculations showed in run 3LM3-10, indicating that the phasing of the peaks is stable.

The last run, 3LM3-14, for this model is performed by taking k_{10}= k_{11}=0.5. Oscillations were recorded after 10000-time units. We see a splitting of PRR7/9 and CCA/LHY oscillations, but not for TOC1 and GI oscillations. The same behavior is shown by Pokhilko et al. 2010 both experimentally and by calculations, yet the oscillations for GI and TOC1 has not been shown.

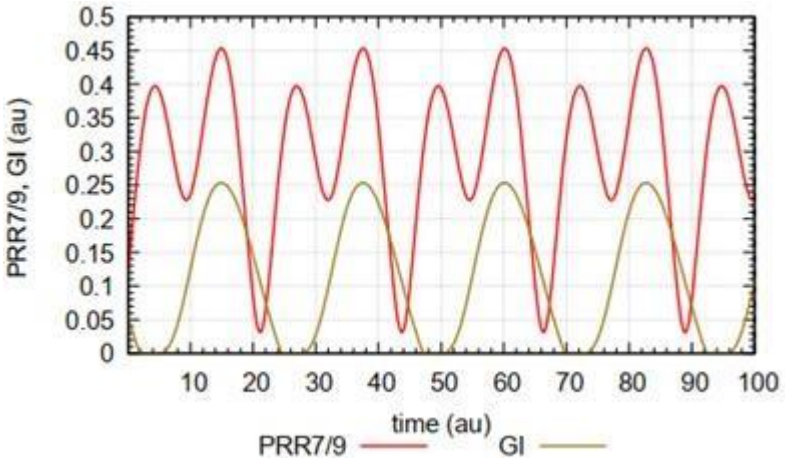

Figure 3-27. The splitting in oscillation is shown by PRR7/9 and CCA/LHY while TOC1 and GI shows regular oscillations. CCA/LHY and TOC1 oscillations not shown.

3.4 Model 3LM4

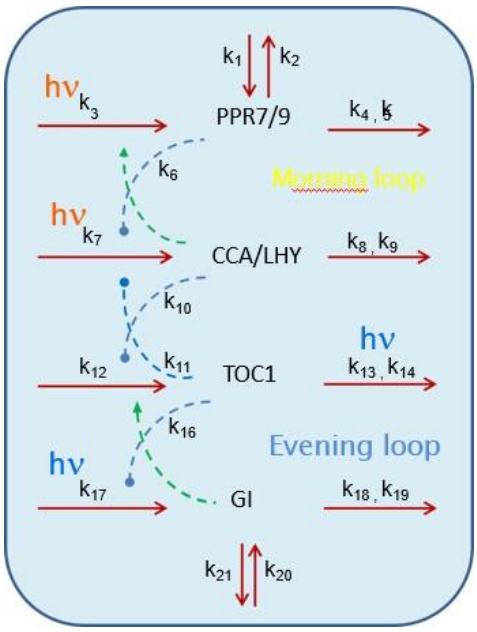

Figure 3-28. The same model as 3LM3but with light input.

This model is used to check the influence of light on the circadian rhythm. The light input is provided on four rate constants and represented by hv. Morning and evening loops are coupled with positive feedback loop while TOC1 and GI has mutual interaction as

The rate equations for this model are the same as model 3LM3. In this model, it is assumed that some rate constants are influenced by light like k3, k7, k13, and k17.in the form

$$k_i = k_{iD} + k_{iL} \cdot \frac{LI}{k_{LI} + LI}$$

Where k_{iD} is a constant dark level and $k_{iL} \cdot \frac{LI}{k_{LI}+LI}$ is the contribution by light. LI is the change of light intensity for one day. The influence of light can be neglected by setting the factor k_{iL} to zero. The impact of light can also be ignored by setting the – sign instead of positive.

The first run 3LM4-01 is taken without impact of light. Each of the oscillators has an estimated period of 20 hours in isolation. The coupling between the oscillators is relatively strong with of k_{10}= k_{11}=0.1. The period of the couple system is 32 hours.

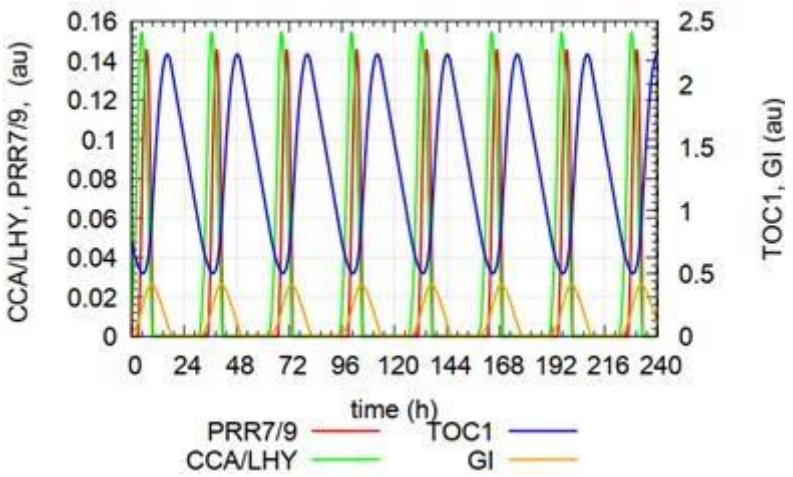

Figure 3-29. Representing the period length slightly less than 24 hours.

The run is performed by further strengthening the coupling by setting k_{10}= k_{11}=0.01. The oscillations for the morning oscillators are wholly suppressed in this case. The morning oscillator oscillates yet with a very low amplitude. The reason for this change can be that the coupling between oscillators is not symmetrical. The morning loop has double inhibition, both external and internal, in comparison to the evening loop oscillator, which has only outer inhibition that is from CCA/LHY.

The mutual inhibition was a bit weakened in strength by replacing the value for k_{10}= k_{11}=0.2. The evening oscillator shows natural oscillations, but oscillations of morning oscillator are complex determined both by TOC1 and GI. One can see that PRR7/9 has low amplitude at the same point when TOC1 has quite a high peak.

Keeping the same value for k_{10}= k_{11}=0.2, next run is performed for 2000 hours and then the concentrations at this time (at t=2000) are used as initial concentrations for this run. The result shows that the intricate oscillating pattern of morning oscillator is stable. Once again keeping k_{10}= k_{11}=0.2, the oscillation pattern was tested after 2000 hours. Regular oscillations appear

for both oscillators in this case. The periods are closer to the free-running periods, which indicate that the coupling might be weak now, yet intricate pattern shown in the beginning by morning oscillators depicts that the coupling however exits.

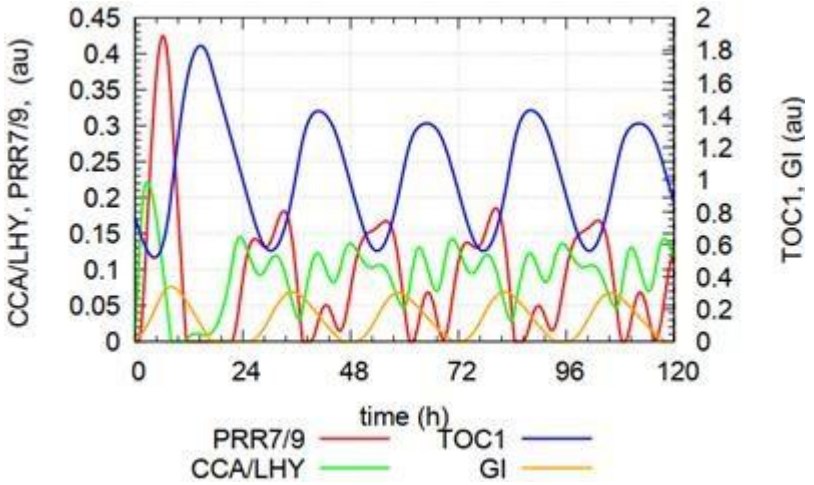

Figure 3-30. Morning oscillator showing complex pattern of oscillations determined by TOC1 and GI. At high TOC1 level PRR7/9 is low.

Increasing the value of k_{10}= k_{11} to 0.5 cause beating in morning loop oscillations without affecting the amplitude of evening oscillator. A further increase up to 10 cause increase in the beating frequency of the morning oscillator. However, the beating of morning oscillator stopped when k_{10}= k_{11}=20.

The next run was performed with k_{3D}=1.5 k_{3L}=2.5. external light period is 24 hours. k_3 is described as follows.

$$k_3 = k_{3D} + k_{3L} \cdot \frac{LI}{10^3 + LI}$$

Where LI=(LIGHTIN)= $1 \times 10^{-3} + 1 \cdot 6 \times 10^5 e^{(-0.078(t-12)^{2.55})}$

With these parameters, the light entrains the morning and evening oscillators with its 24 hours. The phasing of the different components is as described by Nohales and Kay as in the following Figure 3-31.

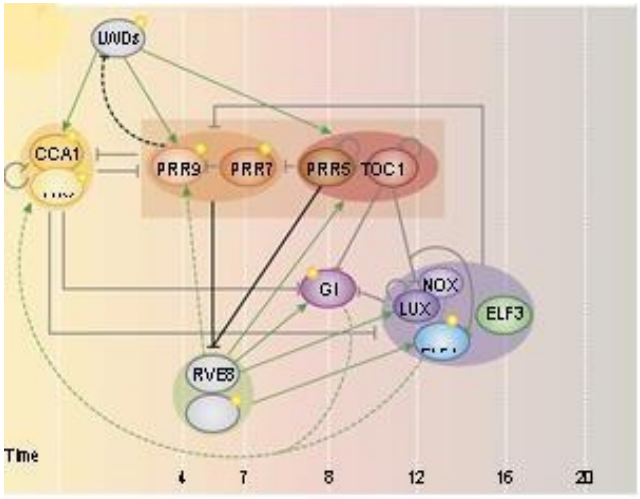

Figure 3-31. The phasing of components of circadian rhythm presented by Nohales and Kay (141).

CCA/LHY peak appears at dawn, followed by PRR7/9 peak. GI peak starts to emerge before GI while TOC1 finally appears in the afternoon (141).

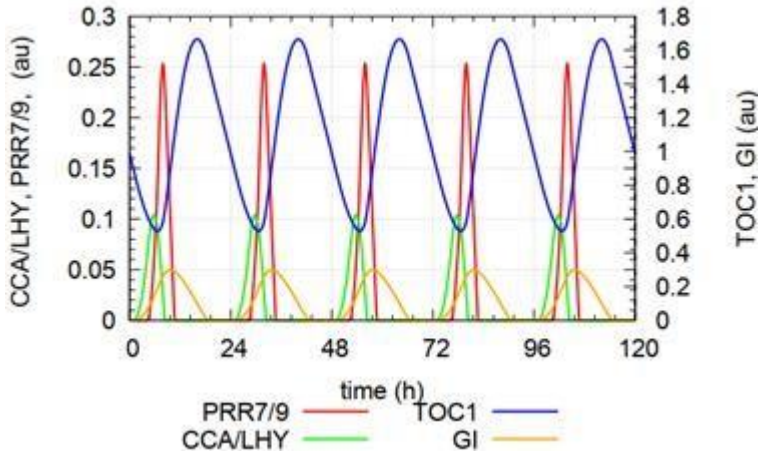

Figure 3-32. The phasing of components of circadian rhythm is in accordance with figure 2 described by Nohales and Kay (141).

3LM4-11 was performed with k_{3D}=1.5 and k_{3L}=0, i.e., no influence of light. Relative phasing was observed in this result, which indicates that the loop structure with their inhibitions/activations determines the relative phasing. The presence of light increases the amplitude of PRR7/9, but the amplitudes of CCA1/LHY, TOC1 and GI are little affected.

The period in the absence of light is 26 hours, more significant than 24 hours period.

For the next run, the light affects only k_7 with k_{7D}=1 and k_{7L}=0.5. Although the light synchronizes morning and evening oscillators to a period of 24 hours, yet all the peaks appear much late and TOC1 peak is the first one to be seen. CCA/LHY does not have a peak in the morning.

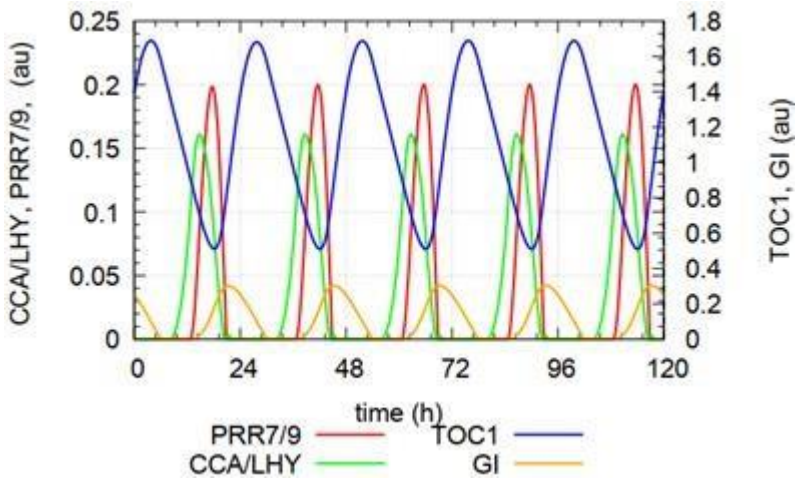

Figure 3-33. By assuming light influence only on k7, the first peak is now appearing to be that of TOC1 while CCA/LHY peak shifts in the afternoon.

In the further run, it was tried to lock the oscillators to a regular 24-hour rhythm by setting the 24-hour light pulses to k_{17}. Locking into 48-hour rhythm oscillations were observed with an additional small peak. In the last run for this model, it was made possible to entrain the system to 24 hours by choosing the appropriate k_{17D} and k_{17L} values. However, due to large k17 values, the evening oscillator suppresses the morning loop oscillators, i.e., the values of CCA/LHY and PRR7/9 are shallow.

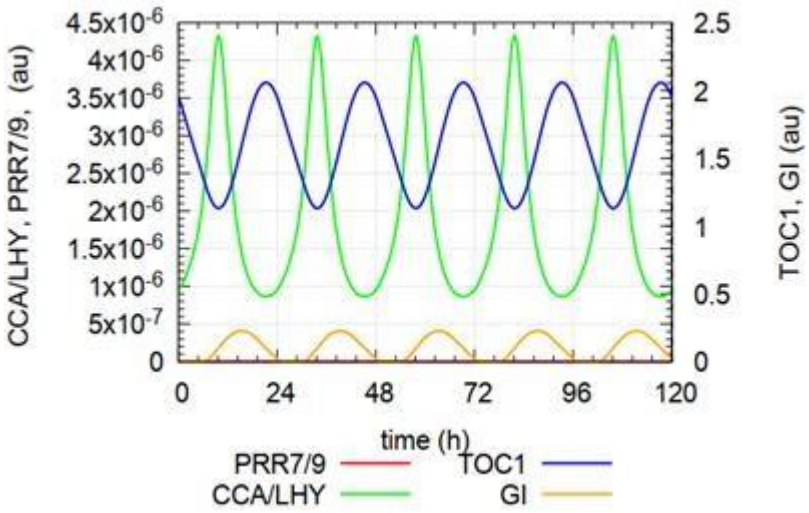

Figure 3-34. Suppression of morning loop oscillator by evening loop components is evident to entrain the system to 24 hours by increasing k_{17}.

Hence PRR7/9, CCA/LHY, TOC1 and GI should probably be interpreted as one functional group as Nohales and Kay (141). Although the overexpression of LHY by PRR7/9 has yet to be investigated.

3.5 Model 3LM41

This model is then further tested to check the influence of light in all three phases with $k_i = k_{iD} + k_{iL} \cdot \frac{LI}{k_{LI}+LI}$ as described in model 3LM4.

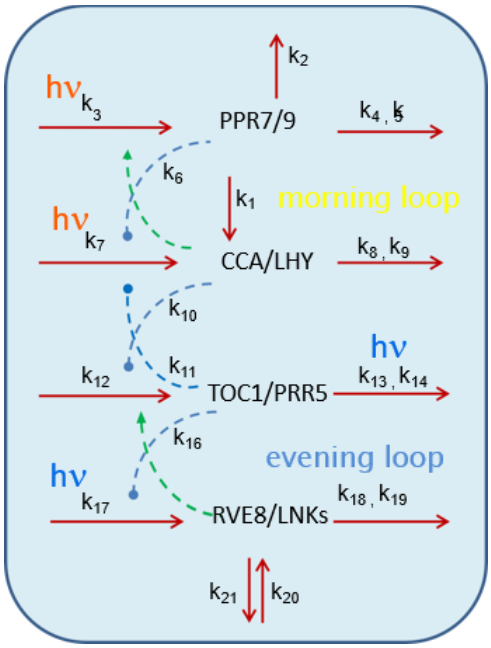

Figure 3-35. The model is an altered form of 3LM4 to check the impact of light which is applied successively.

Besides, the period of environmental light can be changed for each phase. In the last model 3LM4, the effect of single light input pathways on the relative phasing of the few group components was tested. For simplicity, RVE8/LNKs notation is used instead of GI to run the program.

With the model given in Figure 3-35, the investigation was carried out to check how the impact of light successively alters the phasing of the group components. Four runs are performed using different values of parameters, from 3LM41-01 to 3LM41-04. The light input is provided first only on one rate constant k_3 while in the next run light input is given to both k_3 and k_7. The light input is provided to a greater number of components in the next runs. The overview of the phasing of each group, exposed to the same light rhythm is shown in Figure 3-35. There is no

mentionable difference in period length observed in these outputs. The phasing is seen in accordance with that described in Figure 3-31(141).

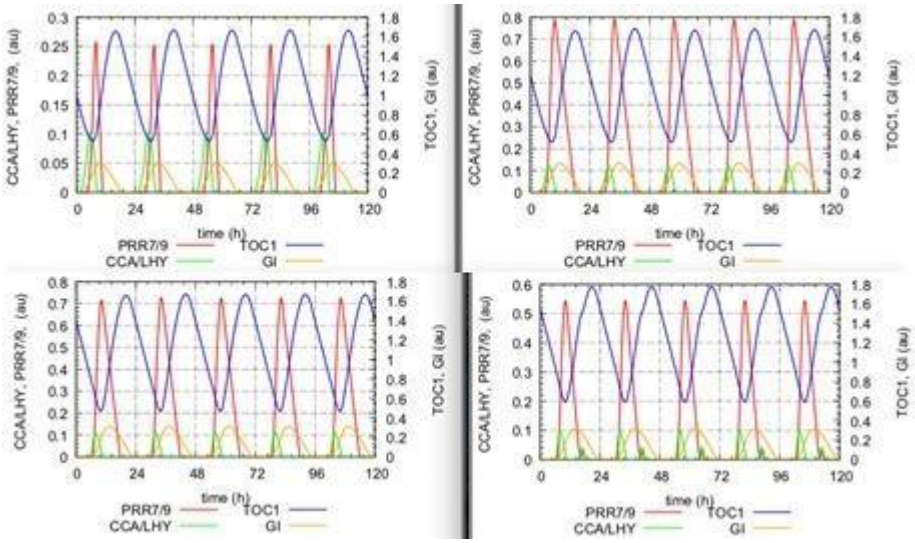

Figure 3-36. Comparison of light influence on components of morning and evening oscillators. The change.

3.6 Model 3LM42

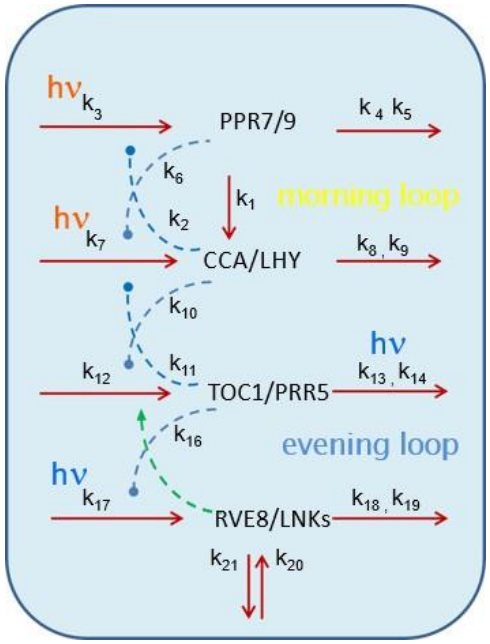

Figure 3-37. The idea of inhibition of PRR7/9 production by CCA/LHY as presented by Adams (150) is taken into notice.

In this version of clock model its assumed that PRR7/9 and CCA/LHY has mutual repression as also indicated in the paper by Adams (150). For simplicity, RVE8/LNKs notation is used instead of GI to run the program. Slight change is made in the rate equation PRR7/9 where

$k_3 \cdot CCA/LHY$ is replaced with

$$k_3 \cdot \frac{k_2}{(k_2 + CCA/LHY)}$$

where k_2 is the inhibition constant.

The run has the k_{3D} =1.5 and k_{3L}=2.5 while all other k_{iL}=0. Also, initial concentration is the same as for the run 3LM41-01. The first run for both models is compared to run 3LM41-01 and 3LM42-01. Since the PRR7/9-CCA/LHY loop is no longer negative, PRR7/9 and TOC1 suppress both CCA/LHY which oscillate at a level around $5x10^{-9}$, which PRR7/9 oscillates around 25.

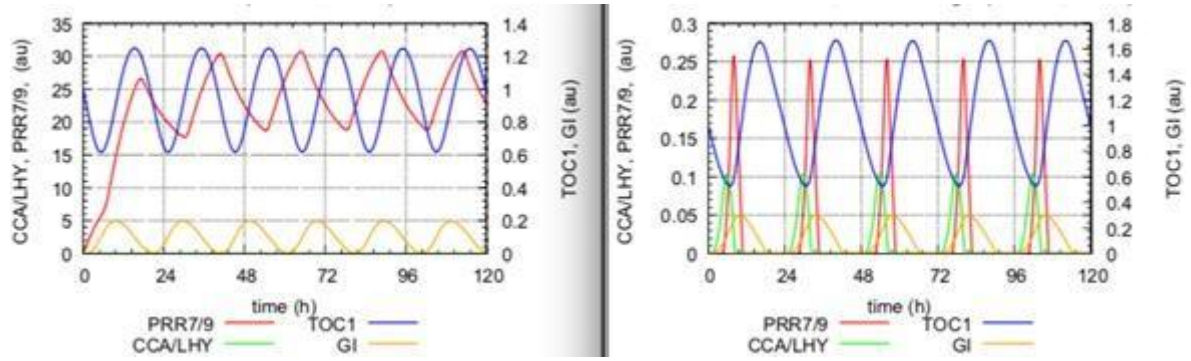

Figure 3-38. The two plots compare 3LM42-01 and 3LM41-01. PRR7/9 and TOC1 suppress CCA/LHY as PRR7/9-CCA/LHY is no longer a negative loop.

As a result of the low CCA/LHY value, the morning and evening loops are practically uncoupled, which is shown in the short period of the evening oscillator. The figure/plot below shows this behavior of uncoupled morning and evening oscillators.

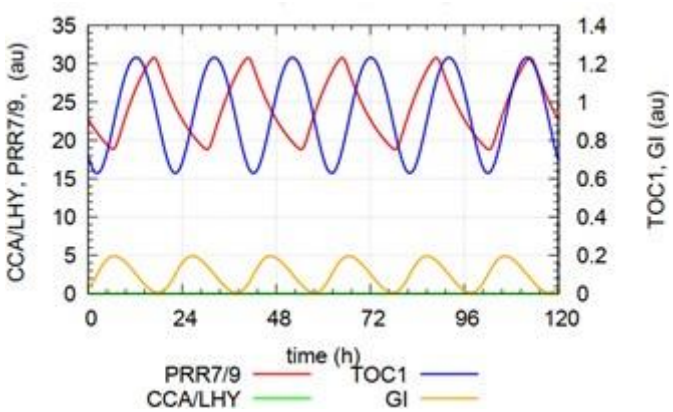

Figure 3-39. Morning and evening oscillators are uncoupled shown by the shorter period of evening oscillator.

It is inevitable that light will entrain the evening loop. In this calculation, all four light dependent pathways are activated but with slightly different rate constants as done in the previous run 3LM41-04. One observes that the phasing is correct, but CCA/LHY oscillates still at a deficient level. In a TOC1 knockout model, one would have the positive feedback of the CCA/LHY, which may be entrained by light but would not be able to oscillate autonomously. Lastly, this was seen that the decoupling of both loops did not have any change what was observed in previously done calculations. This model seems unlikely as the value of CCA/LHY is practically zero. Such wiring between the components of morning loops is nearly impossible.

3.7 Model 3LM44

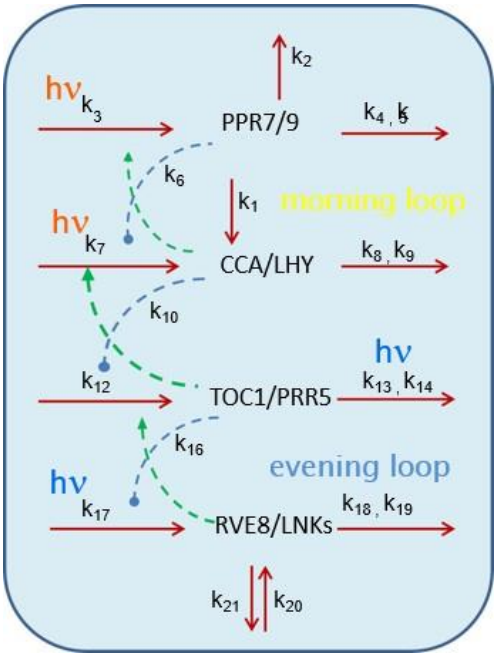

Figure 3-40. This model is based on the idea that positive feedback loop exists between morning and evening oscillators.

Model 3LM44 has a negative regulation between morning and evening oscillators for negative feedback loop. The same interlinked relation was described in Locke's model (84). The relationship between the component of morning and evening oscillators is same as given for model 3LM41. The model is designed to check first PRR7/9 oscillator in isolation that the period of the isolated oscillator matches that of 24-hour rhythms which are given as an input to the two oscillators. For this purpose, the loops are isolated and presented as the following rate equations. For simplicity, RVE8/LNKs notation is used instead of GI to run the program.

Rate equations for morning loop

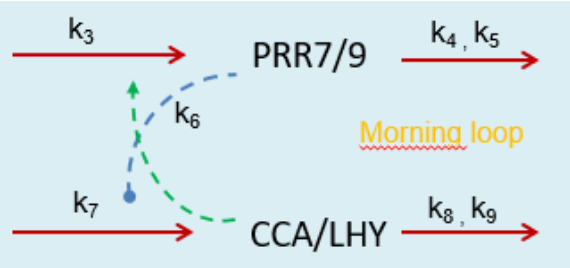

Figure 3-41. Morning loop showing positive feedback loop.

$$\dot{PRR7/9} = k_3 CCA/LHY - k_4 = CCA/LHY_{ss} = \frac{k_4}{k_3}$$

$$\dot{CCA/LHY} = \frac{k_6 k_7}{k_6 + PRR7/9} - k_8 = \frac{k_4 k_7}{k_8} - k_6 = PRR7/9$$

$$\ddot{CCA/LHY} = \frac{-k_6 k_7}{(k_6 + PRR7/9)^2} \dot{PRR7/9} = \frac{-k_6 k_7}{(k_6 + PRR7/9)^2} (k_3 CCA/LHY - k_4)$$

$$= \frac{-k_3 k_6 k_7}{(k_6 + PRR7/9)^2} CCA/LHY + \frac{k_6 k_7 k_4}{(k_6 + PRR7/9)^2}$$

$$\ddot{CCA/LHY} + \frac{-k_3 k_6 k_7}{(k_6 + PRR7/9)^2} CCA/LHY = \frac{k_6 k_7 k_4}{(k_6 + PRR7/9)^2}$$

$$\frac{d}{dt} = \dot{CCA/LHY} = 0 => \left(\frac{1}{k_6 + PRR7/9}\right)^2 = \left(\frac{k_8}{k_6 k_7}\right)^2$$

$$\frac{\frac{\ddot{CCA/LHY}}{k_3 k_6 k_7}}{(k_6 + PRR7/9)^2} + CCA/LHY = \frac{k_4}{k_3} = (CCA/LHY)_{set}$$

Thus, RVE8/LNKs oscillator added its set point

$$\frac{k_4}{k_3} = (CCA/LHY)_{set}$$

$$\omega^2 = k_3 k_6 k_7 \left(\frac{k_8^2}{k_6^2 k_7^2}\right) = \frac{k_3 k_8^2}{k_6 k_7}$$

$$P = \frac{2\pi}{\omega} = \frac{2\pi}{k_8}\sqrt{\frac{k_6 k_7}{k_3}}$$

Rate equations for evening loop

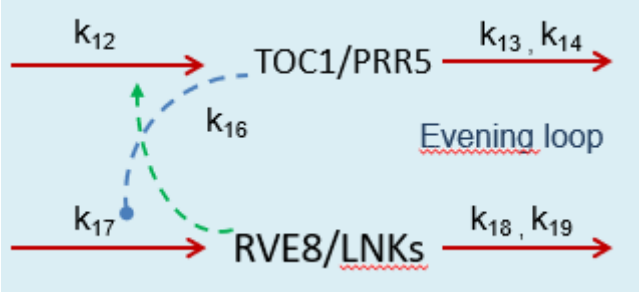

Figure 3-42. An activation of TOC1/PRR5 is taken as kept for previous model.

$$\dot{TOC1/PRR5} = k_{12}RVE8/LNKs - k_{13}$$

$$\dot{RVE8/LNKs} = \frac{k_{17}k_{16}}{k_{16} + TOC1/PRR5} - k_{18}$$

$$\ddot{RVE8/LNKs} = \frac{-k_{17}k_{16}}{(k_{16} + TOC1/PRR5)^2}\dot{TOC1/PRR5}$$

$$= \frac{-k_{16}k_{17}}{(k_{16} + TOC1/PRR5)^2}(k_{12}RVE8/LNKs - k_{13})$$

$$\ddot{RVE8/LNKs} + \frac{-k_{12}k_{16}k_{17}}{(k_{16} + TOC1/PRR5)^2}RVE8/LNKs = \frac{k_{13}k_{16}k_{17}}{(k_{16} + TOC1/PRR5)^2}$$

$$\frac{\frac{\ddot{RVE8/LNKs}}{k_{12}k_{16}k_{17}}}{(k_{16} + TOC1/PRR5)^2} + RVE8/LNKs = \frac{k_{13}}{k_{12}} = RVE8/LNKs_{set}$$

$$\frac{d}{dt} = \dot{TOC1/PRR5} = 0 =>$$

$$\frac{k_{16}k_{17}}{(k_{16} + TOC1/PRR5)} = k_{18}$$

$$(\frac{1}{k_{16} + TOC1/PRR5})^2 = (\frac{k_{18}}{k_{16}k_{17}})^2$$

$$\frac{k_{16}k_{17}}{k_{18}} - k_{16} = TOC1/PRR5ss$$

$$P = \frac{2\pi}{\omega} = \frac{2\pi}{\frac{k_{12}k_{16}k_{17}\,k_{18}^2}{k_{16}^2k_{17}^2}}$$

$$P = \frac{2\pi}{k_{18}}\sqrt{\frac{k_{16}k_{17}}{k_{12}}}$$

In the first run for this model, the morning and evening oscillators are decoupled, running with their period lengths. The theoretically estimated periods agree well with the numerically computed periods, yet there are some differences. Level of CCA/LHY can be influenced by k_3 and k_4. k_4 will not change the period of the morning oscillator, but its average level by increasing k_4. To testify this assumption, the next calculation is done by increasing the value of k_4 to 0.8.

Oscillations are changed in shape and their amplitude, but the period of the morning oscillations id affected from 16.2 to 18.2 hours, numerically. Another attempt was made to adjust the periods for both loops together with the light impact pathways to approximately 24 hours. In outcome, significant alternation in PRR7/9 amplitude was seen, which then was avoided by reducing the value of k_3 to 0.8.

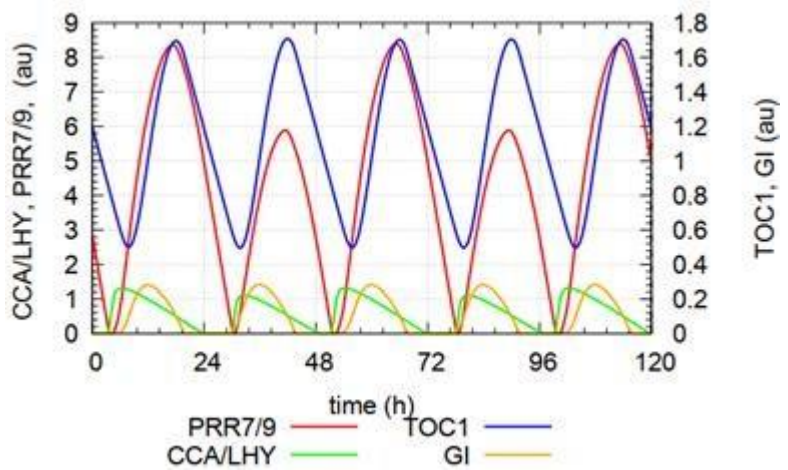

Figure 3-43. Uncoupled morning and evening oscillators are depicted with PRR7/9 amplitude keeps alternating.

The morning and evening loops are coupled after that and waited if the oscillations become fully entrained. However, the phasing is different from that of the 3LM41-01. It can be considered that different light inputs may influence the phasing. Nevertheless, the light input was omitted through k_{13} such that now light input is applied to k_3 and k_7. The phasing remains the same as in the previous run indicating that k_{13} does not have any significant impact.

Subsequently, the light impact was tested again by keeping input only through k_3; for this case, oscillations show an increased period of about 48 hours in relationship to the entraining 24 hours external light cycle. This is apparent in the following Figure 3-44.

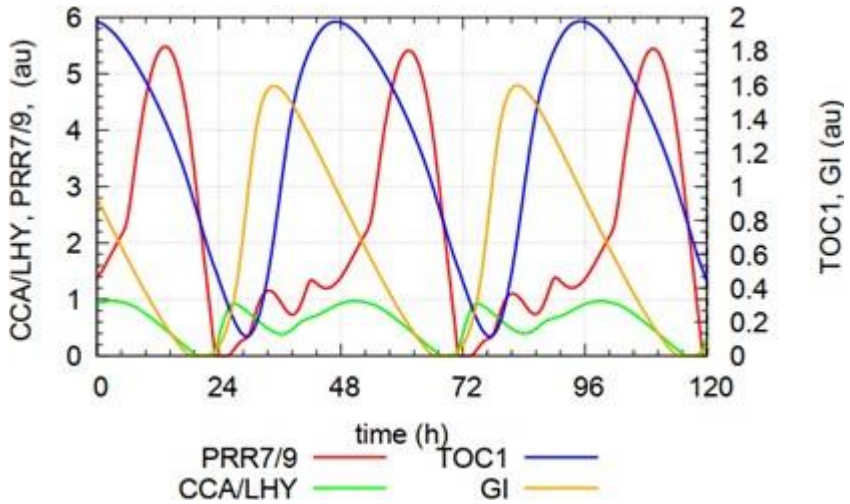

Figure 3-44. A significant increase in period length with complex but regular oscillations by other components.

Although both oscillators when decoupled have a period of 24 hours. If coupled but without any input of light, the period of the couple in-phase oscillations is almost 20 hours. The relative phasing, however, is similar, as seen in the presence of light input. This was also concluded that in light input, most of the responses have chaotic character (Figure not shown).

3.8 Model 3LM45

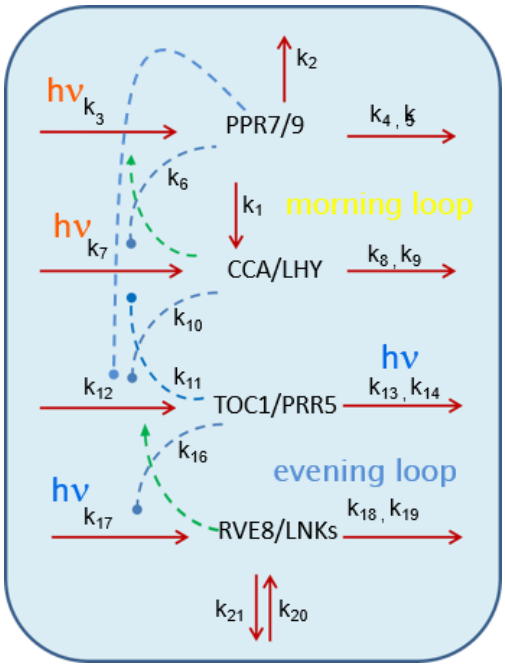

Figure 3-45. Model showing an extra inhibition on TOC1/PRR5 by PRR7/9.

The model 3LM45 is a modification of 3LM41. For simplicity, RVE8/LNKs notation is used instead of GI to run the program. This model has an additional inhibition reaction from PRR7/9 to TOC1/PRR5. This additional repression of the "j_{12}" leads to an increase in the period as indicated by the P formula for 3LM44.

$$j12 = \frac{k_{12}}{k_{10} + CCA/LHY} \cdot \frac{1}{k_{10} + PRR7/9}$$

$$P = \frac{2\pi}{k_{18}} \sqrt{\frac{k_{16} k_{17}}{k_{12}}}$$

The first run for this model was performed with the same rate constants as 3LM41-01, but light input was ignored. Despite the considerable period, the relative phasing of the components is the same as seen for 3LM41. Some of the rate constants were modified to make the approximate period length of 24 hours. Taking into consideration figure 3 in data compiled by Pokhilko (149), where a reduction in the inhibition of PRR9 by TOC1 given a short period, the value of k_3 was increased in the run 3LM45-03 from 1.5 to 2. As a result, reduction in the period was observed as expected from the estimated period of the morning oscillator.

$$P = \frac{2\pi}{\omega} = \frac{2\pi}{k_8} \sqrt{\frac{k_6 k_7}{k_3}}$$

Decoupling of the oscillators resulted in each of the morning and evening oscillator having a period of 14 and 17 hours, respectively, as seen in figure 6-35. Once again, both the oscillators were coupled with slightly different rate constants but neglecting the impact of light. It caused the previous shoulder in CCA/LHY to become less pronounced (not shown).

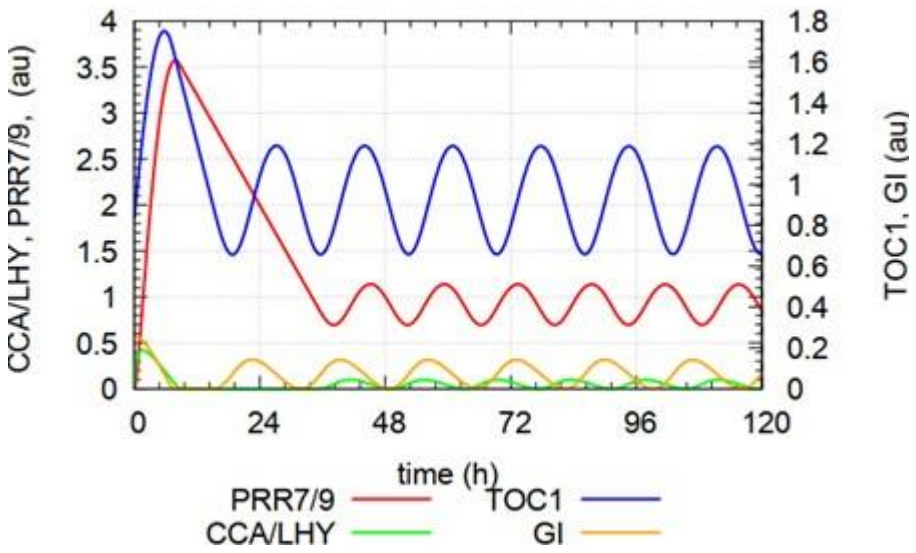

Figure 3-46. Morning and evening oscillators are decoupled and have different period lengths.

4 Discussion

Arabidopsis thaliana circadian clock is composed of different sets of genes that work in positive or negative relationship. Such components also help to entrain the plant according to the external environmental conditions. There have been contradictions in this matter observed in various research papers. In *Arabidopsis thaliana,* components of the circadian oscillator express on different time. CIRCADIAN CLOCK ASSOCIATED 1 (CCA1) and LATE ELONGATED HYPOCOTYL (LHY) are closely related MYB-like transcription factors that are expressed near dawn; which regulate the expression of a suite of PSEUDORESPONSE REGULATOR (PRR) genes, GIGANTEA (GI) and evening complex (EC) members (LUX, ELF3, and ELF4). PRRs are expressed starting from PRR9, PRR7, PRR5 ending at TOC1 (59, 146, 151). Previously it was shown that CCA1 and LHY activate the expression of PRR9 and PRR7, however, recent evidences show that CCA1 and LHY directly suppress PRR7 (96) and PRR9 expression rather than activating them. Additionally, CCA1 and LHY repress the expression of later-expressed genes including PRR5 and TOC1 (150, 152-154). Another task was considered to find out the pattern of appearance of different genes in circadian clock. PRRs genes are sequentially expressed and repress the transcription of CCA1 and LHY, as well as their own transcription from after dawn until near the next dawn. Genetic mutation and transgenic overexpression of TOC1 has provided a controversial picture of the role of TOC1 in the core regulation of CCA1 and LHY expression. Previously, it was determined by using *toc1* mutant plants that TOC1 is positively regulating the morning expression of CCA1 and LHY (46), but later using TOC1 over expressor plants it was shown that TOC1 is directly repressing the expression of CCA and LHY (111, 132). An important suggestion is to find answer that how TOC1 can both repress CCA1/LHY but also be necessary for their transcription activation in the morning. Mostly the rhythmic oscillations are observed with regular pattern for each model starting from 3LM3 till 3LM45. Sometimes chaotic pattern of oscillations for some runs. Period of phases is also seen in accordance with the previous models presented in research papers. A general pattern of appearance of genes at different time during the day is given in tabular form in Figure 3-47.

Gene name	Gene id	Mutant phenotype	Over expression phenotype	Time of expression	Time of activity	Ref.
LWD1, LWD2	AT1G12910 AT3G26640	Short period		dawn	morning	(Wu et al., 2008)
CCA1	AT2G46830	Short period	Arrhythmic in LL Long period in LD	dawn	dawn	(Alabadí et al., 2001), (Matsushika et al., 2002)
LHY	AT1G01060	Short period	Arrhythmic in LL Long period in LD	dawn	dawn	(Alabadí et al., 2001), (Kim et al., 2003)
RVE8	AT3G09600	Long period	Short period	dawn	Midday	(Rawat et al., 2011)
LNK1 LNK2	AT5G64170 AT3G54500	Long period	No phenotype	dawn	Midday	(Xie et al., 2014)
PRR9	AT2G46790	Long period		After down	Morning	(Farré et al., 2005)
PRR7	AT5G02810	Long period		Morning	Midday	(Farré et al., 2005)
PRR5	AT5G24470	Short period	Short period	Afternoon	Afternoon	(Fujiwara et al., 2008), (FUJIMORI et al., 2005)
PRR3	AT5G60100	Short period	Long period	Evening	Evening	(Para et al., 2007)
PRR1	AT5G61380	Short period	Arrhythmic	Evening	Evening	(Alabadí et al., 2001), (Gendron et al., 2012)
LUX1	AT3G46640	Arrhythmic		Evening	Evening	(Nusinow et al., 2011)
ELF4	AT2G40080	Arrhythmic	Long period	Evening	Evening	(Herrero et al., 2012)
ELF3	AT2G25930	Arrhythmic	Long period	Evening	Evening	(Herrero et al., 2012)
GI	AT1G22770	Short period		Evening	Evening	(Dalchau et al., 2011)
ZTL	AT5G57360	Long period	Short period	Evening	Evening	(Somers et al., 2004)

Figure 3-47. Arabidopsis thaliana clock genes expression/translation timing and their mutant phenotype.

5 Conclusion and perspectives

With clocks of all eukaryotes, plant circadian clocks share a typical architecture: interlocked negative feedback loops. Like many eukaryotic clocks, plant clocks use a variety of transcriptional and post-transcription regulatory systems to develop a robust oscillation that is resistant to variability in the environment, yet communicative to ecological time signals.

However, their intricacy differentiates plant clocks from other eukaryotic clocks. Scientific evidence shows that the complex nature of the plant circadian oscillator increases the retention of vigorous rhythms across a wide range of atmospheric conditions. Disordered circadian structure lowers plant growth and endurance, providing the supposition that optimizing circadian function will increase crop productive capacity, especially in plants grown across wide latitudinal ranges.

This is observed by calculations that the phasing in almost every above proposed model for circadian clock remains uniform even if the signaling is altered. The sequence of expression of different genes of Arabidopsis thaliana clock seem to have similar phase of appearance during the day as described recently by Nohales and Kay in 2016. The calculations performed indicate that there can be needed to include other components in the circadian system to explore the complex signaling pathways. It seems that LHY/CCA mutual repression is not experimentally justified and may lead to negative results. This can be interesting if LHY/CCA should be taken as separate components and be tested if there is autoregulation between these genes. It can be said that there lies something unexplored which is needed to completely describe this relationship between genes. A genuine problem is observed if a negative feedback is assumed to exist between morning and evening oscillators. In this case the system collapse and this relation seems to be practically impossible. While enormous progress has been made towards explaining the molecular characteristics and design of the plant circadian oscillator, key mechanistic links for suitable network comprehension remain to be addressed. The task now and in the coming years will be to know these tissue-specific arrangements and to integrate that understanding into current models.

6 References

1. Dunlap JC, Loros JJ, DeCoursey PJ. Chronobiology: biological timekeeping: Sinauer Associates; 2004.
2. Bunning E. The physiological clock. Acad Press New York. 1964.
3. Millar AJ, Kay SA. Circadian control of cab gene transcription and mRNA accumulation in Arabidopsis. The Plant Cell. 1991;3(5):541-50.
4. Millar AJ, Kay SA. The genetics of phototransduction and circadian rhythms in Arabidopsis. BioEssays. 1997;19(3):209-14.
5. Somers DE, Devlin PF, Kay SA. Phytochromes and cryptochromes in the entrainment of the Arabidopsis circadian clock. Science. 1998;282(5393):1488-90.
6. Devlin PF, Kay SA. Cryptochromes are required for phytochrome signaling to the circadian clock but not for rhythmicity. The Plant Cell. 2000;12(12):2499-509.
7. Millar AJ, Kay SA. Integration of circadian and phototransduction pathways in the network controlling CAB gene transcription in Arabidopsis. Proceedings of the National Academy of Sciences. 1996;93(26):15491-6.
8. Covington MF, Panda S, Liu XL, Strayer CA, Wagner DR, Kay SA. ELF3 modulates resetting of the circadian clock in Arabidopsis. The Plant Cell. 2001;13(6):1305-16.
9. Allen T, Koustenis A, Theodorou G, Somers DE, Kay SA, Whitelam GC, et al. Arabidopsis FHY3 specifically gates phytochrome signaling to the circadian clock. The Plant Cell. 2006;18(10):2506-16.
10. Dunlap JC. Genetic analysis of circadian clocks. Annual review of physiology. 1993;55(1):683-728.
11. Pittendrigh CS, Daan S. A functional analysis of circadian pacemakers in nocturnal rodents. Journal of comparative physiology. 1976;106(3):223-52.
12. Aschoff J. Comparative physiology: diurnal rhythms. Annual review of physiology. 1963;25(1):581-600.
13. Salomé PA, McClung CR. PSEUDO-RESPONSE REGULATOR 7 and 9 are partially redundant genes essential for the temperature responsiveness of the Arabidopsis circadian clock. The Plant Cell. 2005;17(3):791-803.
14. Dodd AN, Salathia N, Hall A, Kévei E, Tóth R, Nagy F, et al. Plant circadian clocks increase photosynthesis, growth, survival, and competitive advantage. Science. 2005;309(5734):630-3.
15. Canon WB. The wisdom ofthe body. London: Kegan Paul; 1932.
16. Carpenter R. Homeostasis: a plea for a unified approach. Advances in Physiology Education. 2004;28(4):180-7.
17. Guyton AC. Textbook of medical physiology. 8th. WB Saunders Company, Philadelphia. 1991:782.
18. Davies KJ. Adaptive homeostasis. Molecular aspects of medicine. 2016;49:1-7.
19. Wiener N. Cybernetics or Control and Communication in the Animal and the Machine (Vol. 25). MIT Press doi. 1961;10:13140-000.
20. Wang L, Lee Y-K, Bundman D, Han Y, Thevananther S, Kim C-S, et al. Redundant pathways for negative feedback regulation of bile acid production. Developmental cell. 2002;2(6):721-31.
21. Schwarz M, Lund EG, Lathe R, Björkhem I, Russell DW. Identification and characterization of a mouse oxysterol 7α-hydroxylase cDNA. Journal of Biological Chemistry. 1997;272(38):23995-4001.
22. Conrad M, Hubold C, Fischer B, Peters A. Modeling the hypothalamus–pituitary–adrenal system: homeostasis by interacting positive and negative feedback. Journal of biological physics. 2009;35(2):149-62.
23. Haydon MJ, Román Á, Arshad W. Nutrient homeostasis within the plant circadian network. Frontiers in plant science. 2015;6:299.
24. Johnson CH, Knight MR, Kondo T, Masson P, Sedbrook J, Haley A, et al. Circadian oscillations of cytosolic and chloroplastic free calcium in plants. Science. 1995;269(5232):1863-5.
25. Love J, Dodd AN, Webb AA. Circadian and diurnal calcium oscillations encode photoperiodic information in Arabidopsis. The Plant Cell. 2004;16(4):956-66.
26. Haydon MJ, Bell LJ, Webb AA. Interactions between plant circadian clocks and solute transport. Journal of experimental botany. 2011;62(7):2333-48.
27. Webb AA. The physiology of circadian rhythms in plants. New Phytologist. 2003;160(2):281-303.
28. Merrow M, Boesl C, Ricken J, Messerschmitt M, Goedel M, Roenneberg T. Entrainment of the Neurospora circadian clock. Chronobiology international. 2006;23(1-2):71-80.

29. Heintzen C, Liu Y. The Neurospora crassa circadian clock. Advances in genetics. 2007;58:25-66.
30. Diernfellner AC, Schafmeier T, Merrow MW, Brunner M. Molecular mechanism of temperature sensing by the circadian clock of Neurospora crassa. Genes & development. 2005;19(17):1968-73.
31. Hardin PE. The circadian timekeeping system of Drosophila. Current biology. 2005;15(17):R714-R22.
32. Pittendrigh CS. On temperature independence in the clock system controlling emergence time in Drosophila. Proceedings of the National Academy of Sciences of the United States of America. 1954;40(10):1018.
33. Konopka RJ, Benzer S. Clock mutants of Drosophila melanogaster. Proceedings of the National Academy of Sciences. 1971;68(9):2112-6.
34. Bargiello TA, Young MW. Molecular genetics of a biological clock in Drosophila. Proceedings of the National Academy of Sciences. 1984;81(7):2142-6.
35. Njus D, McMurry L, Hastings J. Conditionality of circadian rhythmicity: synergistic action of light and temperature. Journal of comparative physiology. 1977;117(3):335-44.
36. Millar AJ, Carre IA, Strayer CA, Chua N-H, Kay SA. Circadian clock mutants in Arabidopsis identified by luciferase imaging. Science. 1995;267(5201):1161-3.
37. Bünning E. Known and unknown principles of biological chronometry. Annals of the New York Academy of Sciences. 1967;138(2):515-24.
38. Lecharny A, Schwall M, Wagner E. Stem Extension Rate in Light-Grown Plants: Effects of Photo- and Thermoperiodic Treatments on the Endogenous Circadian Rhythm in Chenopodium rubrum. Plant physiology. 1985;79(3):625-9.
39. Dowson-Day MJ, Millar AJ. Circadian dysfunction causes aberrant hypocotyl elongation patterns in Arabidopsis. The Plant Journal. 1999;17(1):63-71.
40. Nozue K, Covington MF, Duek PD, Lorrain S, Fankhauser C, Harmer SL, et al. Rhythmic growth explained by coincidence between internal and external cues. Nature. 2007;448(7151):358.
41. Yazdanbakhsh N, Sulpice R, Graf A, Stitt M, Fisahn J. Circadian control of root elongation and C partitioning in Arabidopsis thaliana. Plant, Cell & Environment. 2011;34(6):877-94.
42. Niinuma K, Someya N, Kimura M, Yamaguchi I, Hamamoto H. Circadian rhythm of circumnutation in inflorescence stems of Arabidopsis. Plant and cell physiology. 2005;46(8):1423-7.
43. Wang Z-Y, Kenigsbuch D, Sun L, Harel E, Ong MS, Tobin EM. A Myb-related transcription factor is involved in the phytochrome regulation of an Arabidopsis Lhcb gene. The plant cell. 1997;9(4):491-507.
44. Schaffer R, Ramsay N, Samach A, Corden S, Putterill J, Carré IA, et al. The late elongated hypocotyl mutation of Arabidopsis disrupts circadian rhythms and the photoperiodic control of flowering. Cell. 1998;93(7):1219-29.
45. Kim JY, Song HR, Taylor BL, Carré IA. Light-regulated translation mediates gated induction of the Arabidopsis clock protein LHY. The EMBO journal. 2003;22(4):935-44.
46. Alabadí D, Oyama T, Yanovsky MJ, Harmon FG, Más P, Kay SA. Reciprocal regulation between TOC1 and LHY/CCA1 within the Arabidopsis circadian clock. Science. 2001;293(5531):880-3.
47. Alabadí D, Yanovsky MJ, Más P, Harmer SL, Kay SA. Critical role for CCA1 and LHY in maintaining circadian rhythmicity in Arabidopsis. Current Biology. 2002;12(9):757-61.
48. Perales M, Más P. A functional link between rhythmic changes in chromatin structure and the Arabidopsis biological clock. The Plant Cell. 2007;19(7):2111-23.
49. Johansson M. The circadian clock in annuals and perennials: coordination of Growth with Environmental Rhythms: Umeå Universitet, Institutionen för fysiologisk botanik; 2010.
50. Millar AJ, Short SR, Chua N-H, Kay SA. A novel circadian phenotype based on firefly luciferase expression in transgenic plants. The Plant Cell. 1992;4(9):1075-87.
51. Anderson SL, Teakle GR, Martino-Catt SJ, Kay SA. Circadian clock-and phytochrome-regulated transcription is conferred by a 78 bp cis-acting domain of the Arabidopsis CAB2 promoter. The Plant journal: for cell and molecular biology. 1994;6(4):457-70.
52. Millar AJ. Biological clocks in Arabidopsis thaliana. The New Phytologist. 1999;141(2):175-97.
53. Bünning E. Endogenous daily rhythms as the basis of photoperiodism. Ber Deut Bot Ges. 1936;54:590-607.
54. Pittendrigh CS, Minis DH. The entrainment of circadian oscillations by light and their role as photoperiodic clocks. The American Naturalist. 1964;98(902):261-94.
55. Garner WW, Allard HA. Effect of the relative length of day and night and other factors of the environment on growth and reproduction in plants. Monthly Weather Review. 1920;48(7):415-.

56. Franklin KA, Quail PH. Phytochrome functions in Arabidopsis development. Journal of experimental botany. 2009;61(1):11-24.
57. Hearn TJ, Ruiz MCM, Abdul-Awal S, Wimalasekera R, Stanton CR, Haydon MJ, et al. BIG regulates dynamic adjustment of circadian period in Arabidopsis thaliana. Plant physiology. 2018;178(1):358-71.
58. Martínez-García JF, Huq E, Quail PH. Direct targeting of light signals to a promoter element-bound transcription factor. Science. 2000;288(5467):859-63.
59. Hsu PY, Harmer SL. Wheels within wheels: the plant circadian system. Trends in plant science. 2014;19(4):240-9.
60. Kozarewa I, Ibáñez C, Johansson M, Ögren E, Mozley D, Nylander E, et al. Alteration of PHYA expression change circadian rhythms and timing of bud set in Populus. Plant molecular biology. 2010;73(1-2):143-56.
61. Yanovsky MJ, Izaguirre M, Wagmaister JA, Gatz C, Jackson SD, Thomas B, et al. Phytochrome A resets the circadian clock and delays tuber formation under long days in potato. The Plant Journal. 2000;23(2):223-32.
62. Yanovsky MJ, Mazzella MA, Whitelam GC, Casal JJ. Resetting of the circadian clock by phytochromes and cryptochromes in Arabidopsis. Journal of biological rhythms. 2001;16(6):523-30.
63. Banerjee R, Batschauer A. Plant blue-light receptors. Planta. 2005;220(3):498-502.
64. Yu J-W, Rubio V, Lee N-Y, Bai S, Lee S-Y, Kim S-S, et al. COP1 and ELF3 control circadian function and photoperiodic flowering by regulating GI stability. Molecular cell. 2008;32(5):617-30.
65. Millar AJ. Input signals to the plant circadian clock. Journal of Experimental Botany. 2004;55(395):277-83.
66. Más P, Kim W-Y, Somers DE, Kay SA. Targeted degradation of TOC1 by ZTL modulates circadian function in Arabidopsis thaliana. Nature. 2003;426(6966):567.
67. Harmon F, Imaizumi T, Gray WM. CUL1 regulates TOC1 protein stability in the Arabidopsis circadian clock. The Plant Journal. 2008;55(4):568-79.
68. Kim W-Y, Fujiwara S, Suh S-S, Kim J, Kim Y, Han L, et al. ZEITLUPE is a circadian photoreceptor stabilized by GIGANTEA in blue light. Nature. 2007;449(7160):356.
69. Savageau MA. Parameter sensitivity as a criterion for evaluating and comparing the performance of biochemical systems. Nature. 1971;229(5286):542.
70. Glass L, Kauffman SA. The logical analysis of continuous, non-linear biochemical control networks. Journal of theoretical Biology. 1973;39(1):103-29.
71. Novak B, Tyson JJ. Modeling the control of DNA replication in fission yeast. Proceedings of the National Academy of Sciences. 1997;94(17):9147-52.
72. Smolen P, Baxter DA, Byrne JH. Mathematical modeling of gene networks. Neuron. 2000;26(3):567-80.
73. Leloup J-C, Gonze D, Goldbeter A. Limit cycle models for circadian rhythms based on transcriptional regulation in Drosophila and Neurospora. Journal of biological rhythms. 1999;14(6):433-48.
74. Ruoff P, Vinsjevik M, Monnerjahn C, Rensing L. The Goodwin model: simulating the effect of light pulses on the circadian sporulation rhythm of Neurospora crassa. Journal of Theoretical Biology. 2001;209(1):29-42.
75. Forger DB, Peskin CS. A detailed predictive model of the mammalian circadian clock. Proceedings of the National Academy of Sciences. 2003;100(25):14806-11.
76. Leloup J-C, Goldbeter A. Toward a detailed computational model for the mammalian circadian clock. Proceedings of the National Academy of Sciences. 2003;100(12):7051-6.
77. Tyson JJ, Hong CI, Thron CD, Novak B. A simple model of circadian rhythms based on dimerization and proteolysis of PER and TIM. Biophysical journal. 1999;77(5):2411-7.
78. Smolen P, Hardin PE, Lo BS, Baxter DA, Byrne JH. Simulation of Drosophila circadian oscillations, mutations, and light responses by a model with VRI, PDP-1, and CLK. Biophysical journal. 2004;86(5):2786-802.
79. Gardner MJ, Hubbard KE, Hotta CT, Dodd AN, Webb AA. How plants tell the time. Biochemical Journal. 2006;397(1):15-24.
80. Young MW, Kay SA. Time zones: a comparative genetics of circadian clocks. Nature Reviews Genetics. 2001;2(9):702.

81. Harmer SL, Panda S, Kay SA. Molecular bases of circadian rhythms. Annual review of cell and developmental biology. 2001;17(1):215-53.
82. Bell-Pedersen D, Cassone VM, Earnest DJ, Golden SS, Hardin PE, Thomas TL, et al. Circadian rhythms from multiple oscillators: lessons from diverse organisms. Nature Reviews Genetics. 2005;6(7):544.
83. Nakamichi N. Molecular mechanisms underlying the Arabidopsis circadian clock. Plant and Cell Physiology. 2011;52(10):1709-18.
84. Locke J, Millar A, Turner M. Modelling genetic networks with noisy and varied experimental data: the circadian clock in Arabidopsis thaliana. Journal of theoretical biology. 2005;234(3):383-93.
85. Eriksson ME, Hanano S, Southern MM, Hall A, Millar AJ. Response regulator homologues have complementary, light-dependent functions in the Arabidopsis circadian clock. Planta. 2003;218(1):159-62.
86. Hall A, Bastow RM, Davis SJ, Hanano S, McWatters HG, Hibberd V, et al. The TIME FOR COFFEE gene maintains the amplitude and timing of Arabidopsis circadian clocks. The Plant Cell. 2003;15(11):2719-29.
87. McWatters HG, Bastow RM, Hall A, Millar AJ. The ELF3zeitnehmer regulates light signalling to the circadian clock. Nature. 2000;408(6813):716.
88. Pujolàs Maset P, Stainback SB. Aprendre junts alumnes diferents: Els equips d'aprenentatge cooperatiu a l'aula: Eumo; 2003.
89. Locke JC, Kozma-Bognár L, Gould PD, Fehér B, Kevei E, Nagy F, et al. Experimental validation of a predicted feedback loop in the multi-oscillator clock of Arabidopsis thaliana. Molecular systems biology. 2006;2(1):59.
90. Zeilinger MN, Farré EM, Taylor SR, Kay SA, Doyle FJ. A novel computational model of the circadian clock in Arabidopsis that incorporates PRR7 and PRR9. Molecular Systems Biology. 2006;2(1):58.
91. Locke JC, Southern MM, Kozma-Bognár L, Hibberd V, Brown PE, Turner MS, et al. Extension of a genetic network model by iterative experimentation and mathematical analysis. Molecular systems biology. 2005;1(1).
92. Roden LC, Song H-R, Jackson S, Morris K, Carre IA. Floral responses to photoperiod are correlated with the timing of rhythmic expression relative to dawn and dusk in Arabidopsis. Proceedings of the National Academy of Sciences. 2002;99(20):13313-8.
93. Millar AJ. A suite of photoreceptors entrains the plant circadian clock. Journal of biological rhythms. 2003;18(3):217-26.
94. Makino S, Matsushika A, Kojima M, Oda Y, Mizuno T. Light response of the circadian waves of the APRR1/TOC1 quintet: when does the quintet start singing rhythmically in Arabidopsis? Plant and Cell Physiology. 2001;42(3):334-9.
95. Yanovsky MJ, Kay SA. Molecular basis of seasonal time measurement in Arabidopsis. Nature. 2002;419(6904):308.
96. Farré EM, Harmer SL, Harmon FG, Yanovsky MJ, Kay SA. Overlapping and distinct roles of PRR7 and PRR9 in the Arabidopsis circadian clock. Current Biology. 2005;15(1):47-54.
97. Fankhauser C, Staiger D. Photoreceptors in Arabidopsis thaliana: light perception, signal transduction and entrainment of the endogenous clock. Planta. 2002;216(1):1-16.
98. Rand D, Shulgin B, Salazar D, Millar A. Design principles underlying circadian clocks. Journal of The Royal Society Interface. 2004;1(1):119-30.
99. Harmer SL, Hogenesch JB, Straume M, Chang H-S, Han B, Zhu T, et al. Orchestrated transcription of key pathways in Arabidopsis by the circadian clock. Science. 2000;290(5499):2110-3.
100. Edwards KD, Akman OE, Knox K, Lumsden PJ, Thomson AW, Brown PE, et al. Quantitative analysis of regulatory flexibility under changing environmental conditions. Molecular systems biology. 2010;6(1):424.
101. Nakamichi N, Kita M, Ito S, Yamashino T, Mizuno T. PSEUDO-RESPONSE REGULATORS, PRR9, PRR7 and PRR5, together play essential roles close to the circadian clock of Arabidopsis thaliana. Plant and Cell Physiology. 2005;46(5):686-98.
102. McClung CR. Plant circadian rhythms. The Plant Cell. 2006;18(4):792-803.
103. Thain SC, Hall A, Millar AJ. Functional independence of circadian clocks that regulate plant gene expression. Current Biology. 2000;10(16):951-6.
104. Doyle MR, Davis SJ, Bastow RM, McWatters HG, Kozma-Bognár L, Nagy F, et al. The ELF4 gene controls circadian rhythms and flowering time in Arabidopsis thaliana. Nature. 2002;419(6902):74.

105. Matsushika A, Yamashino T, Mizuno T, editors. Structure and function of the clock-associated PRR factors in Arabidopsis. Plant and Cell Physiology; 2005: OXFORD UNIV PRESS GREAT CLARENDON ST, OXFORD OX2 6DP, ENGLAND.
106. Matsushika A, Makino S, Kojima M, Mizuno T. Circadian waves of expression of the APRR1/TOC1 family of pseudo-response regulators in Arabidopsis thaliana: insight into the plant circadian clock. Plant and Cell Physiology. 2000;41(9):1002-12.
107. Nakamichi N, Matsushika A, Yamashino T, Mizuno T. Cell autonomous circadian waves of the APRR1/TOC1 quintet in an established cell line of Arabidopsis thaliana. Plant and cell physiology. 2003;44(3):360-5.
108. Fujiwara S, Wang L, Han L, Suh S-S, Salomé PA, McClung CR, et al. Post-translational regulation of the Arabidopsis circadian clock through selective proteolysis and phosphorylation of pseudo-response regulator proteins. Journal of Biological Chemistry. 2008;283(34):23073-83.
109. Farré EM, Kay SA. PRR7 protein levels are regulated by light and the circadian clock in Arabidopsis. The Plant Journal. 2007;52(3):548-60.
110. Ito S, Nakamichi N, Kiba T, Yamashino T, Mizuno T. Rhythmic and light-inducible appearance of clock-associated pseudo-response regulator protein PRR9 through programmed degradation in the dark in Arabidopsis thaliana. Plant and cell physiology. 2007;48(11):1644-51.
111. Makino S, Matsushika A, Kojima M, Yamashino T, Mizuno T. The APRR1/TOC1 quintet implicated in circadian rhythms of Arabidopsis thaliana: I. Characterization with APRR1-overexpressing plants. Plant and Cell Physiology. 2002;43(1):58-69.
112. Nakamichi N, Kiba T, Henriques R, Mizuno T, Chua N-H, Sakakibara H. PSEUDO-RESPONSE REGULATORS 9, 7, and 5 are transcriptional repressors in the Arabidopsis circadian clock. The Plant Cell. 2010;22(3):594-605.
113. Kiba T, Henriques R, Sakakibara H, Chua N-H. Targeted degradation of PSEUDO-RESPONSE REGULATOR5 by an SCFZTL complex regulates clock function and photomorphogenesis in Arabidopsis thaliana. The Plant Cell. 2007;19(8):2516-30.
114. Ito S, Niwa Y, Nakamichi N, Kawamura H, Yamashino T, Mizuno T. Insight into missing genetic links between two evening-expressed pseudo-response regulator genes TOC1 and PRR5 in the circadian clock-controlled circuitry in Arabidopsis thaliana. Plant and cell physiology. 2008;49(2):201-13.
115. Somers DE, Schultz TF, Milnamow M, Kay SA. ZEITLUPE encodes a novel clock-associated PAS protein from Arabidopsis. Cell. 2000;101(3):319-29.
116. Han L, Mason M, Risseeuw EP, Crosby WL, Somers DE. Formation of an SCFZTL complex is required for proper regulation of circadian timing. The Plant Journal. 2004;40(2):291-301.
117. Kevei E, Gyula P, Hall A, Kozma-Bognár L, Kim W-Y, Eriksson ME, et al. Forward genetic analysis of the circadian clock separates the multiple functions of ZEITLUPE. Plant physiology. 2006;140(3):933-45.
118. Baudry A, Ito S, Song YH, Strait AA, Kiba T, Lu S, et al. F-box proteins FKF1 and LKP2 act in concert with ZEITLUPE to control Arabidopsis clock progression. The Plant Cell. 2010;22(3):606-22.
119. Somers DE, Fujiwara S. Thinking outside the F-box: novel ligands for novel receptors. Trends in plant science. 2009;14(4):206-13.
120. Jones MA. Entrainment of the Arabidopsis circadian clock. Journal of Plant Biology. 2009;52(3):202-9.
121. Para A, Farre EM, Imaizumi T, Pruneda-Paz JL, Harmon FG, Kay SA. PRR3 is a vascular regulator of TOC1 stability in the Arabidopsis circadian clock. The Plant Cell. 2007;19(11):3462-73.
122. Mizoguchi T, Wright L, Fujiwara S, Cremer F, Lee K, Onouchi H, et al. Distinct roles of GIGANTEA in promoting flowering and regulating circadian rhythms in Arabidopsis. The Plant Cell. 2005;17(8):2255-70.
123. Park DH, Somers DE, Kim YS, Choy YH, Lim HK, Soh MS, et al. Control of circadian rhythms and photoperiodic flowering by the Arabidopsis GIGANTEA gene. Science. 1999;285(5433):1579-82.
124. Pruneda-Paz JL, Breton G, Para A, Kay SA. A functional genomics approach reveals CHE as a component of the Arabidopsis circadian clock. Science. 2009;323(5920):1481-5.
125. Kuno N, Møller SG, Shinomura T, Xu X, Chua N-H, Furuya M. The novel MYB protein EARLY-PHYTOCHROME-RESPONSIVE1 is a component of a slave circadian oscillator in Arabidopsis. The Plant Cell. 2003;15(10):2476-88.

126. Yanhui C, Xiaoyuan Y, Kun H, Meihua L, Jigang L, Zhaofeng G, et al. The MYB transcription factor superfamily of Arabidopsis: expression analysis and phylogenetic comparison with the rice MYB family. Plant molecular biology. 2006;60(1):107-24.
127. Zhang X, Chen Y, Wang ZY, Chen Z, Gu H, Qu LJ. Constitutive expression of CIR1 (RVE2) affects several circadian-regulated processes and seed germination in Arabidopsis. The Plant Journal. 2007;51(3):512-25.
128. Rawat R, Schwartz J, Jones MA, Sairanen I, Cheng Y, Andersson CR, et al. REVEILLE1, a Myb-like transcription factor, integrates the circadian clock and auxin pathways. Proceedings of the national academy of sciences. 2009;106(39):16883-8.
129. Song H-R, Carré IA. DET1 regulates the proteasomal degradation of LHY, a component of the Arabidopsis circadian clock. Plant molecular biology. 2005;57(5):761-71.
130. David KM, Armbruster U, Tama N, Putterill J. Arabidopsis GIGANTEA protein is post-transcriptionally regulated by light and dark. FEBS letters. 2006;580(5):1193-7.
131. Huang W, Pérez-García P, Pokhilko A, Millar A, Antoshechkin I, Riechmann JL, et al. Mapping the core of the Arabidopsis circadian clock defines the network structure of the oscillator. Science. 2012;336(6077):75-9.
132. Gendron JM, Pruneda-Paz JL, Doherty CJ, Gross AM, Kang SE, Kay SA. Arabidopsis circadian clock protein, TOC1, is a DNA-binding transcription factor. Proceedings of the National Academy of Sciences. 2012;109(8):3167-72.
133. Wang L, Kim J, Somers DE. Transcriptional corepressor TOPLESS complexes with pseudoresponse regulator proteins and histone deacetylases to regulate circadian transcription. Proceedings of the National Academy of Sciences. 2013;110(2):761-6.
134. Rawat R, Takahashi N, Hsu PY, Jones MA, Schwartz J, Salemi MR, et al. REVEILLE8 and PSEUDO-REPONSE REGULATOR5 form a negative feedback loop within the Arabidopsis circadian clock. PLoS genetics. 2011;7(3):e1001350.
135. Rugnone ML, Soverna AF, Sanchez SE, Schlaen RG, Hernando CE, Seymour DK, et al. LNK genes integrate light and clock signaling networks at the core of the Arabidopsis oscillator. Proceedings of the National Academy of Sciences. 2013;110(29):12120-5.
136. Hsu PY, Devisetty UK, Harmer SL. Accurate timekeeping is controlled by a cycling activator in Arabidopsis. Elife. 2013;2:e00473.
137. Xie Q, Wang P, Liu X, Yuan L, Wang L, Zhang C, et al. LNK1 and LNK2 are transcriptional coactivators in the Arabidopsis circadian oscillator. The Plant Cell. 2014;26(7):2843-57.
138. Nakamichi N, Kiba T, Kamioka M, Suzuki T, Yamashino T, Higashiyama T, et al. Transcriptional repressor PRR5 directly regulates clock-output pathways. Proceedings of the National Academy of Sciences. 2012;109(42):17123-8.
139. Pokhilko A, Fernández AP, Edwards KD, Southern MM, Halliday KJ, Millar AJ. The clock gene circuit in Arabidopsis includes a repressilator with additional feedback loops. Molecular systems biology. 2012;8(1):574.
140. Wu J-F, Wang Y, Wu S-H. Two new clock proteins, LWD1 and LWD2, regulate Arabidopsis photoperiodic flowering. Plant physiology. 2008;148(2):948-59.
141. Nohales MA, Kay SA. Molecular mechanisms at the core of the plant circadian oscillator. Nature structural & molecular biology. 2016;23(12):1061.
142. Wu J-F, Tsai H-L, Joanito I, Wu Y-C, Chang C-W, Li Y-H, et al. LWD–TCP complex activates the morning gene CCA1 in Arabidopsis. Nature communications. 2016;7:13181.
143. Mockler T, Michael T, Priest H, Shen R, Sullivan C, Givan S, et al., editors. The DIURNAL project: DIURNAL and circadian expression profiling, model-based pattern matching, and promoter analysis. Cold Spring Harbor symposia on quantitative biology; 2007: Cold Spring Harbor Laboratory Press.
144. Farinas B, Mas P. Functional implication of the MYB transcription factor RVE8/LCL5 in the circadian control of histone acetylation. The Plant Journal. 2011;66(2):318-29.
145. Li G, Siddiqui H, Teng Y, Lin R, Wan X-y, Li J, et al. Coordinated transcriptional regulation underlying the circadian clock in Arabidopsis. Nature cell biology. 2011;13(5):616.
146. McClung CR. The Plant Circadian Oscillator. Biology. 2019;8(1):14.
147. Drengstig T, Jolma I, Ni X, Thorsen K, Xu X, Ruoff P. A basic set of homeostatic controller motifs. Biophysical journal. 2012;103(9):2000-10.
148. Pruneda-Paz JL, Kay SA. An expanding universe of circadian networks in higher plants. Trends in plant science. 2010;15(5):259-65.

149. Pokhilko A, Hodge SK, Stratford K, Knox K, Edwards KD, Thomson AW, et al. Data assimilation constrains new connections and components in a complex, eukaryotic circadian clock model. Molecular systems biology. 2010;6(1):416.
150. Adams S, Manfield I, Stockley P, Carré IA. Revised morning loops of the Arabidopsis circadian clock based on analyses of direct regulatory interactions. PLoS One. 2015;10(12):e0143943.
151. Webb AA, Seki M, Satake A, Caldana C. Continuous dynamic adjustment of the plant circadian oscillator. Nature communications. 2019;10(1):550.
152. Fogelmark K, Troein C. Rethinking transcriptional activation in the Arabidopsis circadian clock. PLoS computational biology. 2014;10(7):e1003705.
153. Kamioka M, Takao S, Suzuki T, Taki K, Higashiyama T, Kinoshita T, et al. Direct repression of evening genes by CIRCADIAN CLOCK-ASSOCIATED 1 in Arabidopsis circadian clock. The Plant Cell. 2016:tpc. 00737.2015.
154. Sanchez SE, Kay SA. The plant circadian clock: from a simple timekeeper to a complex developmental manager. Cold Spring Harbor perspectives in biology. 2016;8(12):a027748.